EARTHQUAKE ENGINEERING RESEARCH CENTER

STABILIZATION OF POTENTIALLY LIQUEFIABLE SAND DEPOSITS USING GRAVEL DRAIN SYSTEMS

by

H. Bolton Seed

John R. Booker

Report No. EERC 76-10

April 1976

A Report on Research Sponsored by
the National Science Foundation

College of Engineering

University of California

Berkeley, California

Stabilization of Potentially Liquefiable Sand Deposits Using Gravel Drain Systems

by

H. Bolton Seed,[1] and John R. Booker[2]

INTRODUCTION

In recent years substantial gains have been made in the understanding of the phenomenon of liquefaction of saturated granular materials. It is now widely accepted that if a saturated granular material is subjected to cyclic loading involving the reversal of shear stresses it will tend to compact, and that if the material is unable to drain, this tendency to decrease in volume will lead to an increase in pore water pressure. Ultimately if the cyclic loading is maintained the soil will reach a condition of zero effective stress and, depending on its relative density, will suffer essentially a complete loss of strength (liquefaction) or undergo some degree of strain with little or no resistance to deformation (initial liquefaction with limited strain potential).

Considerable progress has been made in the development of both tests and test procedures to obtain quantitative measures of the stress conditions which lead to these types of soil liquefaction. This development has been accompanied by an associated development of methods of analysis (Seed and Idriss, 1967, 1971) which make use of the test results to evaluate the liquefaction potential of soil deposits in the field, and the methods have been found to provide a useful basis for assessing probable site performance under prescribed earthquake conditions.

---

[1]Prof. of Civil Engrg., University of California, Berkeley, Calif.

[2]Sr. Lecturer, Dept. of Civil Engrg., University of Sydney, Australia, currently Visiting Scholar, Dept. of Civil Engrg., University of California, Berkeley, Calif.

Much of the work referred to in the preceding paragraph has been restricted to soil behavior under undrained conditions and finds its application in situations in which the redistribution and dissipation of pore water pressure do not have a significant influence on the liquefaction potential of the soil mass. It has been recognized, however, that such mechanisms may be of considerable importance and may have both adverse and beneficial effects. For example, the dissipation of pore water pressures generated in deep soil layers may lead to upward seepage which results in liquefaction of surface layers (Seed and Lee, 1966; Ambraseys and Sarma, 1969; Yoshimi, Yoshiaki and Kuwabara, 1973 and Seed, Martin and Lysmer, 1975). On the other hand, if the pore water pressures generated in a soil mass by cyclic loading can to some extent be dissipated as they are created, then the danger of liquefaction may be averted, Seed et al (1975). In fact it is thought that the better field performance of gravels over sands may be directly attributable to their capacity to dissipate pore water pressures because of their higher permeability (Wong, Seed, and Chan, 1975).

A possible method of stabilizing a soil deposit susceptible to liquefaction is to install a system of gravel or rock drains as shown in Fig. 1(a) so that pore water pressures generated by cyclic loading may be dissipated almost as fast as they are generated. In this paper the one dimensional theory of pore water pressure generation and dissipation developed by Seed, et al(1975) is generalised to three dimensions and applied to the analysis of columnar gravel drains under a variety of earthquake conditions. The results of these analyses are summarised as a series of charts which provide a convenient basis for design considerations.

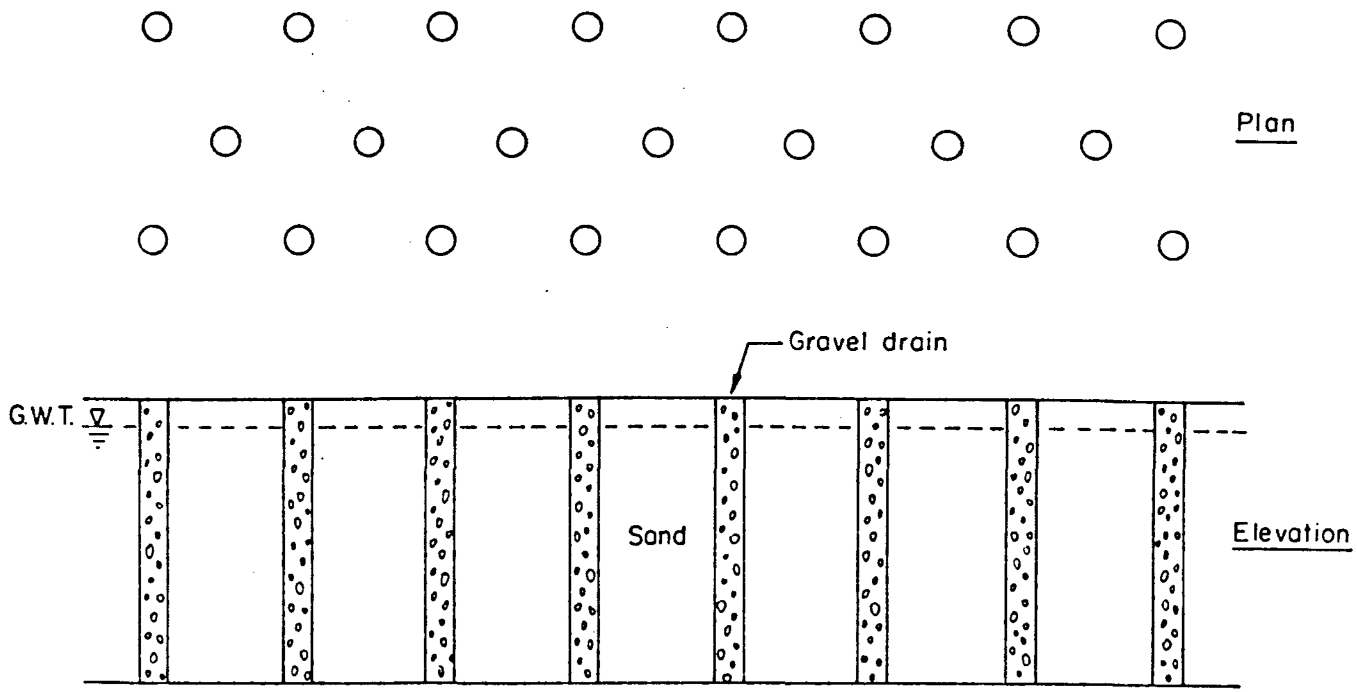

Fig 1(a) ARRANGEMENT OF GRAVEL DRAIN SYSTEM

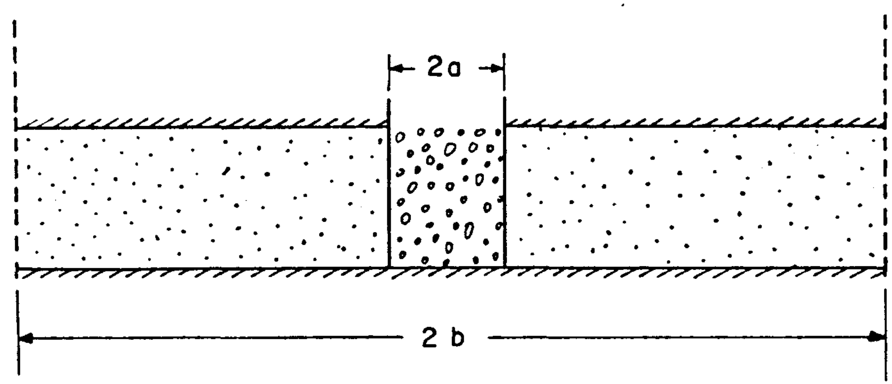

Fig. 1(b) GRAVEL DRAIN WITH RADIAL DRAINAGE ONLY

BASIC EQUATIONS

In developing the basic equations governing the generation and dissipation of pore water pressure throughout a granular material, it will be assumed that the flow of the pore water is governed by Darcy's Law so that the usual considerations of continuity of flow lead to the equation:

$$\frac{\partial}{\partial x}\left(\frac{k_H}{\gamma_\omega}\frac{\partial u}{\partial x}\right) + \frac{\partial}{\partial y}\left(\frac{k_H}{\gamma_\omega}\frac{\partial u}{\partial y}\right) + \frac{\partial}{\partial z}\left(\frac{k_V}{\gamma_\omega}\frac{\partial u}{\partial z}\right) = \frac{\partial \varepsilon}{\partial t} \qquad (1)$$

where u is the excess hydrostatic pore water pressure

k_V, k_H are coefficients of permeability in the vertical and horizontal directions

γ_ω is the unit weight of water

and ε is the volume strain, with volumetric reduction being considered positive.

During an interval of time dt the pore water pressure in an element of soil will undergo a change du, while the element will also be subjected to dN cycles of alternating shear stress which will cause an additional increase in pore pressure $\partial u_g/\partial N \cdot dN$, where u_g is the pore pressure generated by the alternating shear stresses for the appropriate conditions of prior strain history. It therefore follows, considering that the change in bulk stress is negligible, that the volume change $d\varepsilon$ of the element in time dt is given by

$$d\varepsilon = m_{v3}\left(du - \frac{\partial u_g}{\partial N}\, dN\right) \qquad (2a)$$

where m_{v3} is the coefficient of volume compressibility

i.e. $$\frac{\partial \varepsilon}{\partial t} = m_{v3}\left(\frac{\partial u}{\partial t} - \frac{\partial u_g}{\partial N} \cdot \frac{\partial N}{\partial t}\right) \qquad (2b)$$

Combining Eqns. (1) and (2b) it is found that:

$$\frac{\partial}{\partial x}\left(\frac{k_H}{\gamma_\omega}\frac{\partial}{\partial x}\right) + \frac{\partial}{\partial y}\left(\frac{k_H}{\gamma_\omega}\frac{\partial u}{\partial y}\right) + \frac{\partial}{\partial z}\left(\frac{k_H}{\gamma_\omega}\frac{\partial u}{\partial z}\right) = \left[\frac{\partial u}{\partial t} - \frac{\partial u_g}{\partial N}\frac{\partial N}{\partial t}\right] \quad (3)$$

If the coefficients of permeability are constant and the problem exhibits radial symmetry, Eqn. (3) becomes

$$\frac{k_H}{\gamma_\omega m_{V3}}\left(\frac{\partial^2 u}{\partial^2 r} + \frac{1}{r}\frac{\partial u}{\partial r}\right) + \frac{k_V}{\gamma_\omega m_{v3}}\frac{\partial^2 u}{\partial r^2} = \frac{\partial u}{\partial t} - \frac{\partial u_g}{\partial N}\frac{\partial N}{\partial t} \quad (4)$$

and for purely vertical drainage reduces to the form developed by Seed et al (1975).

$$\frac{k_V}{\gamma_\omega m_{v3}}\frac{\partial^2 u}{\partial z^2} = \frac{\partial u}{\partial t} - \frac{\partial u_g}{\partial N}\frac{\partial N}{\partial t} \quad (5)$$

Under conditions of purely radial drainage as considered in the following section, Eqn. (4) reduces to

$$\frac{k_H}{\gamma_\omega m_{V3}}\left(\frac{\partial^2 u}{\partial r^2} + \frac{1}{r}\frac{\partial u}{\partial r}\right) = \frac{\partial u}{\partial t} - \frac{\partial u_g}{\partial N}\frac{\partial N}{\partial t} \quad (6)$$

In order to evaluate the extent of pore pressure generation and dissipation using this equation, it is necessary to determine $\partial u_g/\partial N$ and $\partial N/\partial t$ as well as the soil properties k_H and m_{v3}. The values of $\partial u_g/\partial N$ can be found from undrained tests as described by Seed et al (1975). For many soils the relationship between u_g and N can be expressed for practical purposes in terms of the number of cycles N_ℓ required to cause initial liquefaction under the given stress conditions in the form (Seed et al, 1975):

$$\frac{u_g}{\sigma_o'} = \frac{2}{\pi}\arcsin\left(\frac{N}{N_\ell}\right)^{1/2\alpha} \quad (7)$$

where σ_o' is the initial mean bulk effective stress for triaxial test conditions or the initial vertical effective stress for simple shear conditions and α is an empirical constant which has a typical value of 0.7. (see Fig. 2)

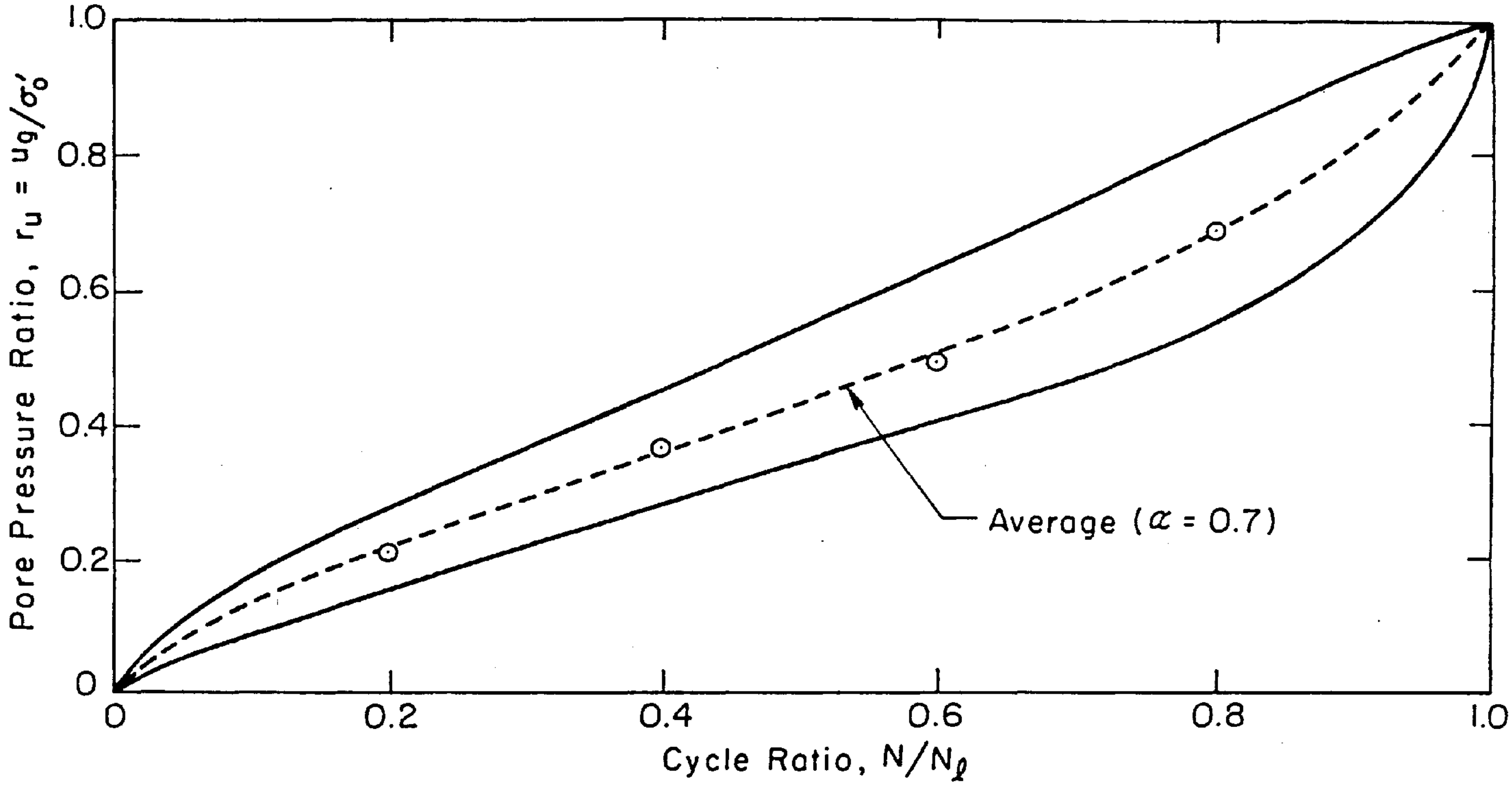

Fig. 2 RATE OF PORE WATER PRESSURE BUILD-UP IN CYCLIC SIMPLE SHEAR TESTS (after De Alba et al.)

Thus,

$$\frac{\partial u_g}{\partial N} = \frac{2\sigma_o'}{\alpha\pi N_\ell} \quad \frac{1}{\sin^{2\alpha-1}(\frac{\pi}{2} r_u) \cos(\frac{\pi}{2} r_u)} \tag{8}$$

where $r_u = \frac{u}{\sigma_o'}$, is the pore pressure ratio.

For practical purposes the irregular cyclic loading induced by an earthquake may be converted to an equivalent number N_{eq} of uniform stress cycles at a stress ratio τ_h/σ_o' occuring in some duration of time t_d of earthquake shaking (Seed, Idriss, Makdisi, Banerjee, 1975). Thus

$$\frac{\partial N}{\partial t} = \frac{N_{eq}}{t_d} \tag{9}$$

In using these results it must be noted that the rate of pore pressure generation $\partial u_g/\partial N$ depends on the previous cyclic history of the soil and this may be represented approximately by the accumulated pore pressure u. Thus for any given point at time t_1, the appropriate rate of pore pressure generation $(\partial u_g/\partial N)_{t_1}$ must be determined from Eqn. (8) corresponding to the value of u existing in the soil at that time. By this means the past history of strain cycles may be taken into account with a reasonable degree of accuracy.

ANALYSIS OF ROCK DRAINS

As discussed previously, in cases of high liquefaction potential the installation of columnar gravel drains may well provide an efficient method for preventing the development of excessively high pore water pressures. In most practical cases for example the horizontal permeability of a sand will be several times greater than its vertical permeability and the spacing between vertical drains can be made less than the distance required for water to drain vertically to a free surface. Furthermore, many natural deposits of sand are interspersed with narrow horizontal layers of relatively impermeable silt which may severely inhibit vertical drainage. For these reasons it seems quite likely that the dominant mechanism in the operation of a gravel drain system will often be one of pure horizontal drainage.

Consider, therefore, a network of rock drains as shown in Fig. 1(b) of diameter 2a and an effective spacing 2b installed in a layer of sand with horizontal permeability, k, an initial effective stress σ_o' and having characteristics such that it would liquefy after N_ℓ uniform stress cycles of magnitude γ_{eq} if it were undrained. Suppose also that the layer is subjected to an earthquake consisting of N_{eq} uniform stress cycles of the same magnitude applied over a period of time t_d. It will be assumed that the pore pressure generating characteristics of the sand are described by Eqn. 9 and that the filler material in the drains is far more permeable than the surrounding sand layer, so that the excess pore water pressure in the drain is effectively zero. It will also be assumed that the coefficient of compressibility is constant. Examination of experimental data (Lee and Albaiso 1974) shows that this is nearly so for moderate pore pressure ratios and thus if the sand drains are performing their function, this assumption is justified.

Under these assumptions of purely radial flow, the pore pressure ratio, $r_u = u/\sigma_o'$, throughout the sand and drain system depends on the following dimensionless parameters:

a/b = a ratio characterizing the geometric configuration of the sand drains

N_{eq}/N_ℓ = a ratio characterizing the severity of the earthquake shaking, in relation to the liquefaction characteristics of the sand,

$T_{bd} \quad = \dfrac{k}{\gamma_\omega} \cdot \dfrac{t_d}{m_{v3} b^2}$ relating the duration of the earthquake to the consolidation properties of the sand,

and α = a parameter characterizing the shape of the pore pressure generation curve, Eqn. 7. (It is found that for many materials $\alpha = 0.7$ fits the experimental data well and this value will be adopted throughout this paper).

A finite element program LARF (Liquefaction Analysis for Radial Flow has been written to solve Eqn. 3 for purely radial flow (see Appendix A).

Before examining the behavior of a gravel drain system it is instructive to consider the behavior of a sand layer when no drain is present. Since only radial drainage is considered and no vertical drainage may occur, the layer will act in an undrained manner. There are two cases to consider. First if the number of equivalent uniform stress cycles induced by the earthquake, N_{eq}, is less than that required to cause liquefaction, N_ℓ, the excess pore water pressure will rise according to Eqn. 7, until a final value (which remains constant thereafter) is reached when $t = t_d$ and $N = N_{eq}$. Of more practical interest is the case when $N_{eq} > N_\ell$. For this case the excess pore water pressure will rise according to Eqn. 7 until it reaches the value σ'_o when $N = N_\ell$ and $t = t_u$ where

$$t_u = \frac{N_\ell}{N_{eq}} \; t_d \tag{10}$$

the sand then developing a condition of initial liquefaction and no further increase in pore pressure being possible.

In order to illustrate the effect of a system of gravel drains, the

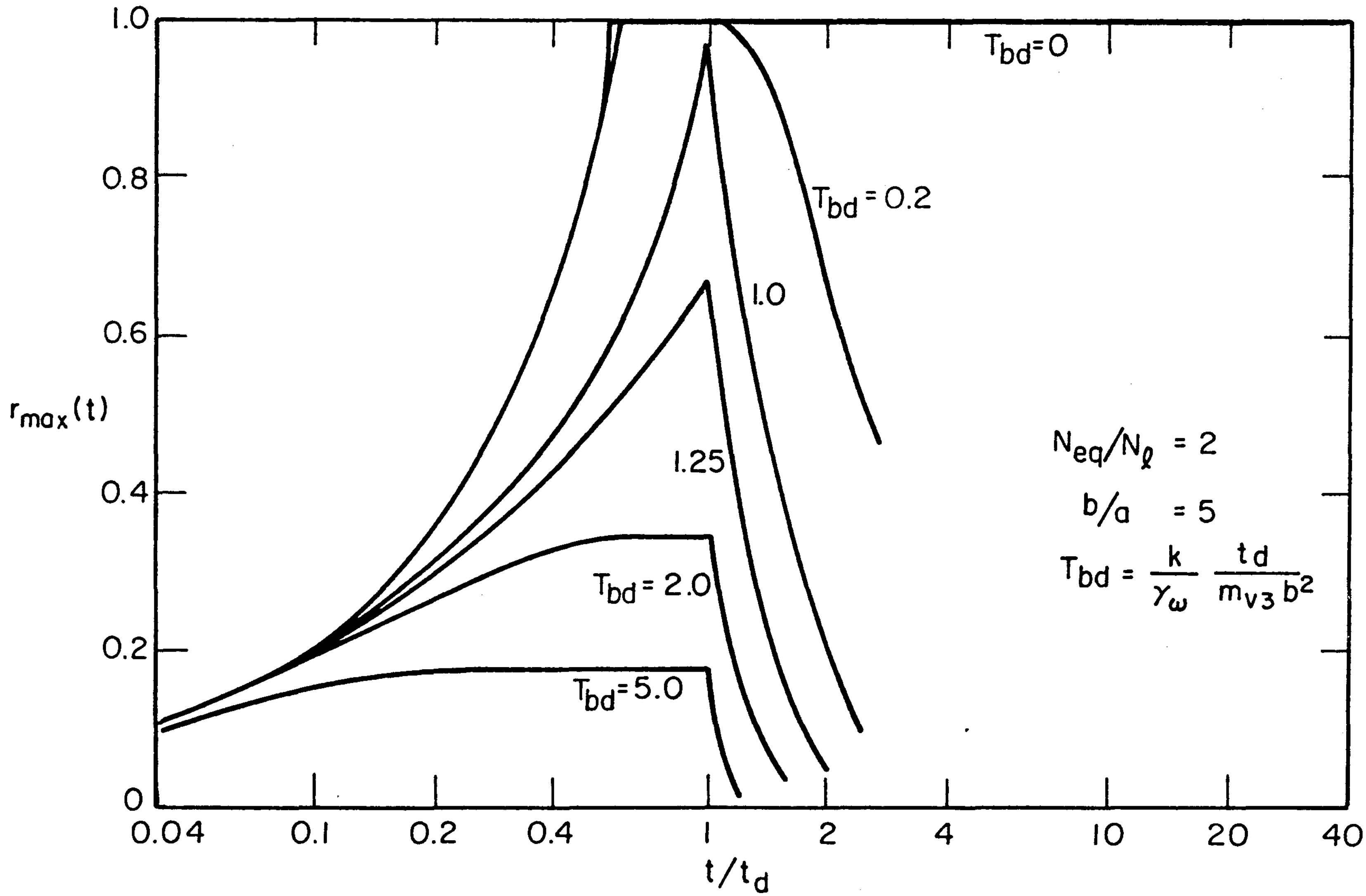

Fig. 3 RELATIONSHIP BETWEEN MAXIMUM PORE PRESSURE RATIO AND TIME

case of a sand layer with drains spaced at $a/b = 0.2$ will be examined in some detail for an earthquake condition where N_ℓ is equal to one half of N_{eq}.

In Fig. 3 the maximum pore pressure ratio $r_{max}(t)$ = maximum value of u/σ_o' throughout the layer at time t is plotted against t/t_d. If the sand had zero permeability so that, $T_{bd} = 0$, undrained conditions would prevail and the pore pressure ratio would rise to a value of 1 at $t = t = t_u = 1/2\ t_d$ (for this case); the entire layer would then develop a condition of initial liquefaction at this instant and remain in this condition thereafter since no dissipation could occur. For a sand having a relatively low permeability coefficient, say for example, a value corresponding to $T_{bd} = 0.2$, the maximum pore pressure ratio rises approximately as it would in the undrained case and initial liquefaction will develop at some time between $t = t_u$ and $t = t_d$. The liquefied zone then continues to grow until the end of strong shaking. After this no further excess pore water pressures are generated, the pore pressures that have built up dissipate and the liquefied zone contracts and finally vanishes whereupon the maximum pore pressure ratio drops steadily from the value one down to zero. If the sand had a still greater permeability, corresponding to say $T_{bd} = 1.25$, the pore pressures build up during the period of strong shaking but the soil does not develop a condition of initial liquefaction although it can be seen that if the earthquake were maintained beyond t_d liquefaction would eventually occur. On cessation of strong shaking the excess pore pressures dissipate and the pore pressure ratio drops from its greatest value r_g back to zero. For a still higher permeability corresponding to $T_{bd} = 5.0$, the pore pressure increases initially but then tends to level off as a stage is reached where the rate of dissipation of pore pressures is almost equal to the rate of their generation.

Similar observations to those described in the previous paragraph hold for a material for which $N_{eq}/N_{\ell} = 5$. This case can be regarded as similar in every respect to the one described previously except that the intensity of the earthquake is increased. This implies that excess pore pressures are generated at a faster rate and thus it would be expected that the permeability necessary to limit the pore pressure ratio to a specified greatest value r_g would be increased. This is illustrated by comparison of the results shown in Figs. 3 and 4.

The effect of changing the diameter of the gravel drain is illustrated by considering a material for which $N_{eq}/N_{\ell} = 2$ for a range of values of a/b but with a constant value of $T_{bd} = 1$. Computed results for this case are shown in Fig. 5. If no drains are present a/b = 0, there are no drainage boundaries and so the layer behaves in an undrained fashion and liquefies at $t = t_u = \frac{1}{2} t_d$ and remains liquefied thereafter. For a relatively small drain corresponding to a/b = 0.1, initial liquefaction is deferred for a period of time but eventually occurs, the liquefied region continuing to grow until the end of the period of strong shaking; thereafter it shrinks and vanishes as a result of pore water pressure dissipation. If a larger diameter drain is introduced corresponding to a/b = 0.25, initial liquefaction of any part of the layer may be prevented entirely and the greatest pore pressure ratio will be less than one. Note that the diameter of the drain in this region of values of a/b is quite critical and the greatest value of pore pressure ratio r_g developed changes rapidly with a/b. Thus, for example, there is a far greater decrease of r_g when a/b changes from 0.2 to 0.25 than there is when a/b changes from 0.25 to 0.3.

In designing a network of gravel drains to prevent liquefaction, it would be helpful to know for a given soil and a given diameter of drain

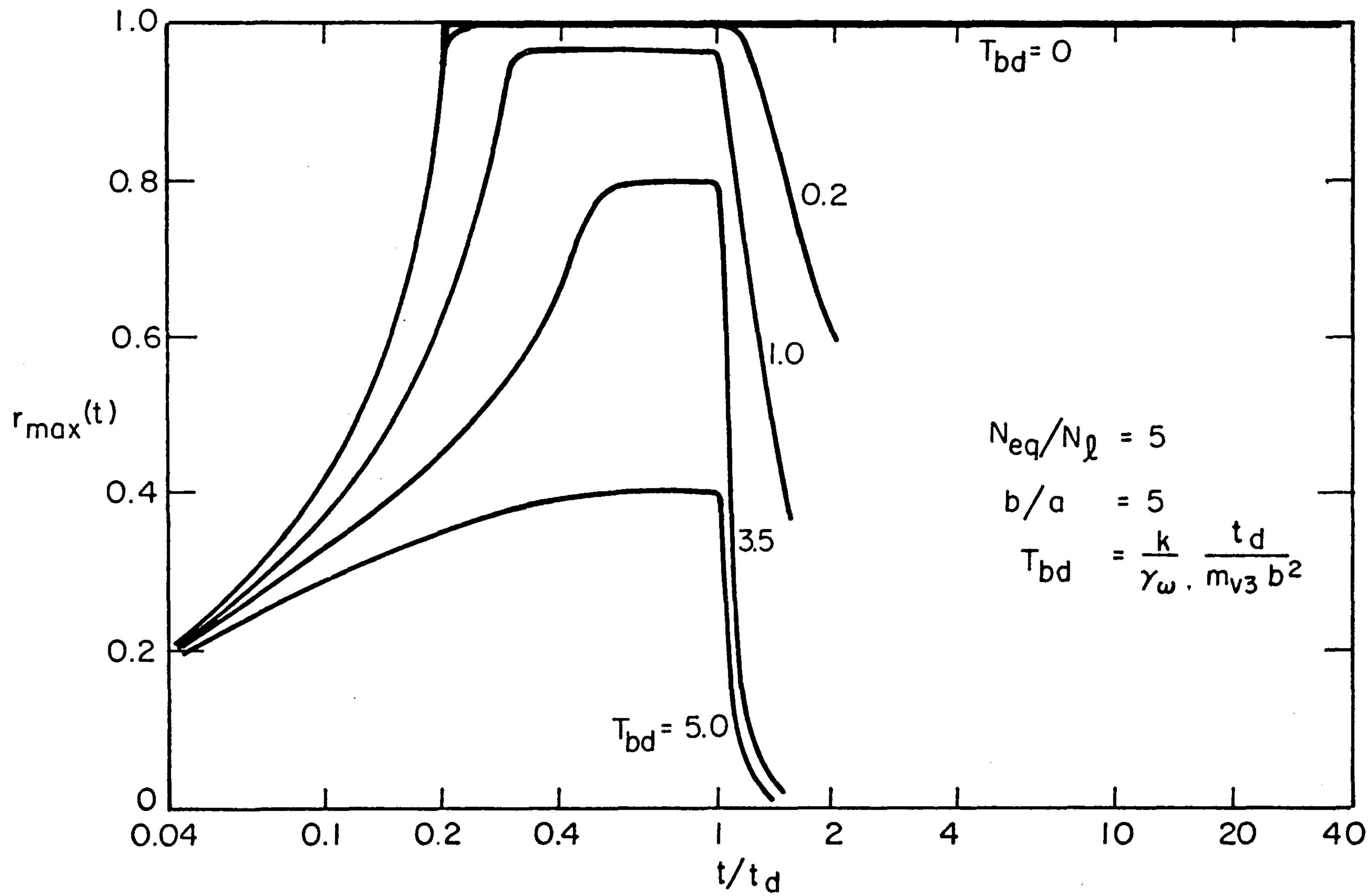

Fig. 4 RELATIONSHIP BETWEEN MAXIMUM PORE PRESSURE RATIO AND TIME

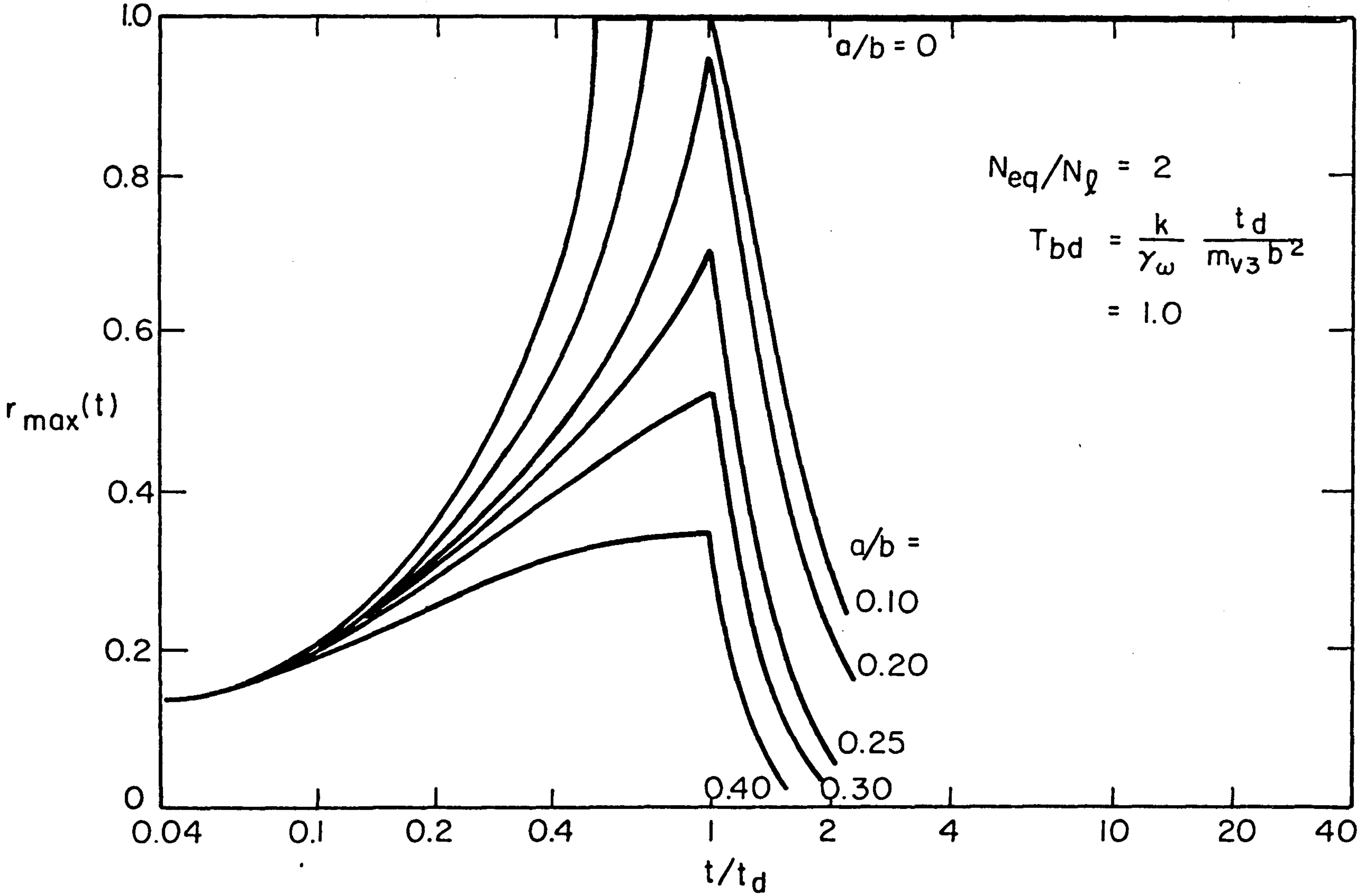

Fig. 5 EFFECT OF DRAIN DIAMETER AND DRAIN SPACING ON MAXIMUM PORE PRESSURE RATIO

what spacing of drains should be chosen to limit the pore pressure ratio to a given greatest value r_g. To facilitate this choice, a series of curves Figs. 6 to 9 have been computed which show the variation of the greatest pore pressure ratio r_g developed as a function of the spacing ratio a/b for values of N_{eq}/N_ℓ equal to 1, 2, 3, 4, and for a range of values of the parameter $T_{ad} = \frac{k}{\gamma_\omega} \cdot \frac{t_d}{m_{v3} a^2}$. For any particular soil and a given diameter of sand drain, N_{eq}/N_ℓ and T_{ad} will be known and thus the value of a/b corresponding to a given allowable value of r_g can be read directly from the curves. A similar series of plots showing the greatest average pore pressure ratio in the soil, $(\bar{r})_g$, are shown in Figs. 10-13.

<u>Example</u>

Suppose, for example, that a soil layer having the properties

$$k = 10^{-5} \text{ m/sec}$$

and

$$m_{v3} = 2 \times 10^{-6} \text{ ft}^2/\text{lb} = 4.2 \times 10^{-5} \text{ kN/m}^2$$

is subjected to an earthquake which can be considered as applying 24 uniform stress cycles in a period of 70 seconds and it is known that under undrained conditions, the soil would liquefy under this sequence of stress applications after 12 cycles (i.e. after 35 seconds) so that $N_{eq}/N_\ell = 2$.

If gravel drains of 2' (0.61 m) diameter were considered then, noting that $\gamma_\omega = 9.8 \text{ kN/m}^3$:

$$T_{ad} = \frac{k}{\gamma_\omega} \cdot \frac{t_d}{m_{v3}\, a^2} = \frac{10^{-5} \times 70}{9.8 \times 4.2 \times 10^{-5} \times (0.305)^2} = 18.3$$

Now referring to Fig. 7, if a value of $r_g = 0.6$ were considered to be allowable, it may be seen that

$$b/a \leq 0.25$$

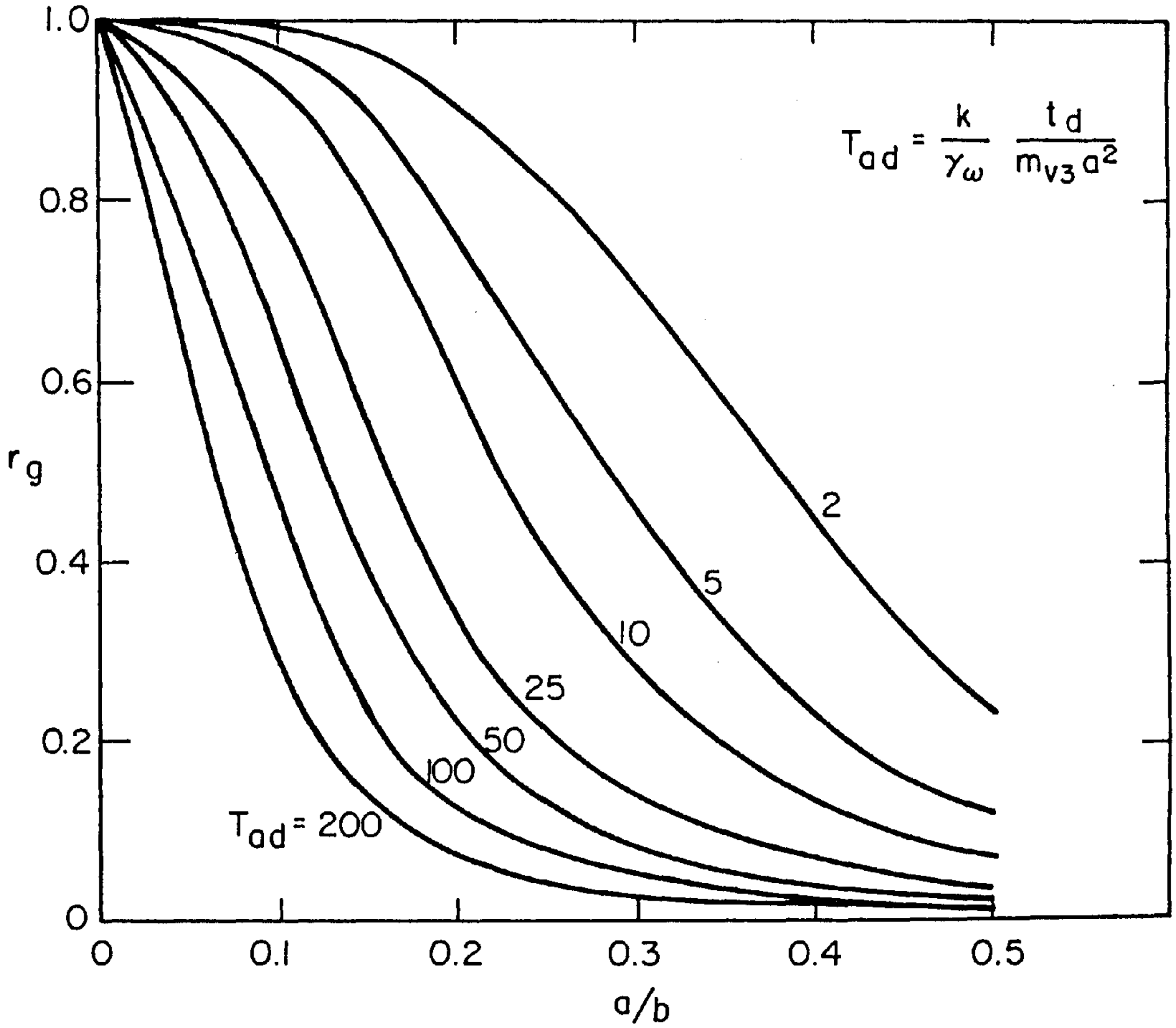

Fig. 6 RELATIONSHIP BETWEEN GREATEST PORE PRESSURE RATIO AND DRAIN SYSTEM PARAMETERS FOR $N_{eq}/N_\ell = 1$

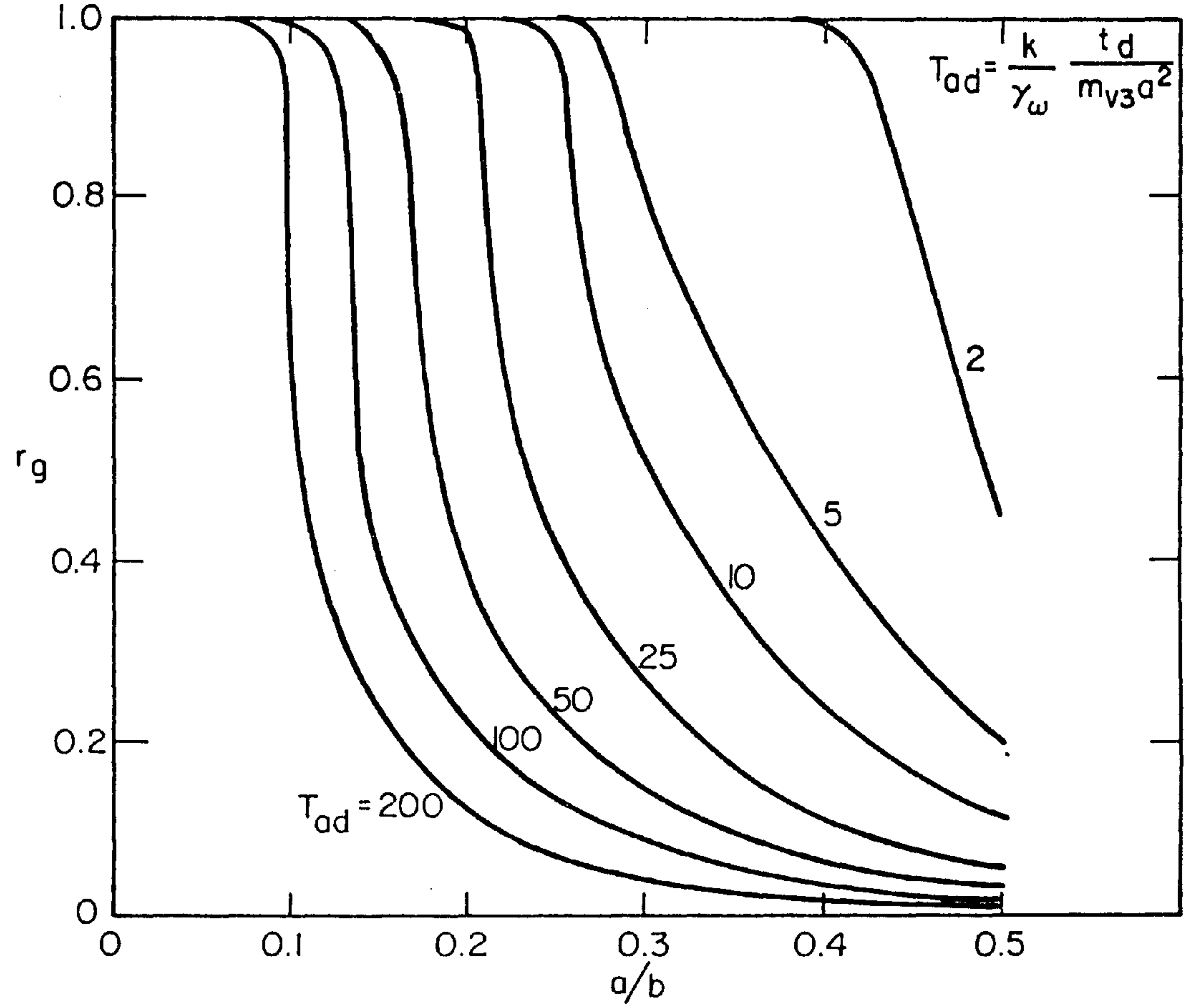

Fig. 7 RELATIONSHIP BETWEEN GREATEST PORE PRESSURE RATIO AND DRAIN SYSTEM PARAMETERS FOR $N_{eq}/N_{\ell} = 2$

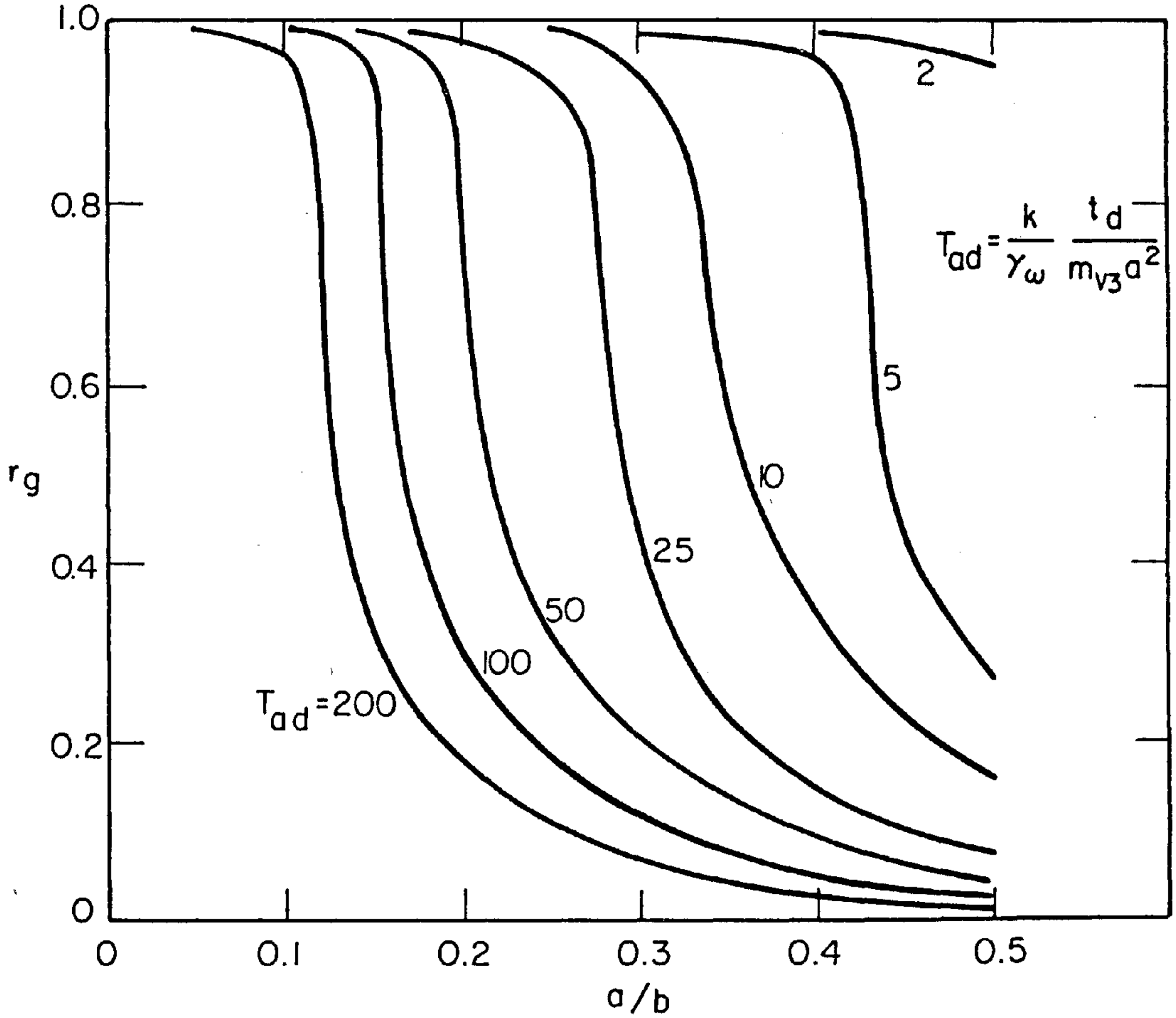

Fig. 8 RELATIONSHIP BETWEEN GREATEST PORE PRESSURE RATIO AND DRAIN SYSTEM PARAMETERS FOR $N_{eq}/N_\ell = 3$

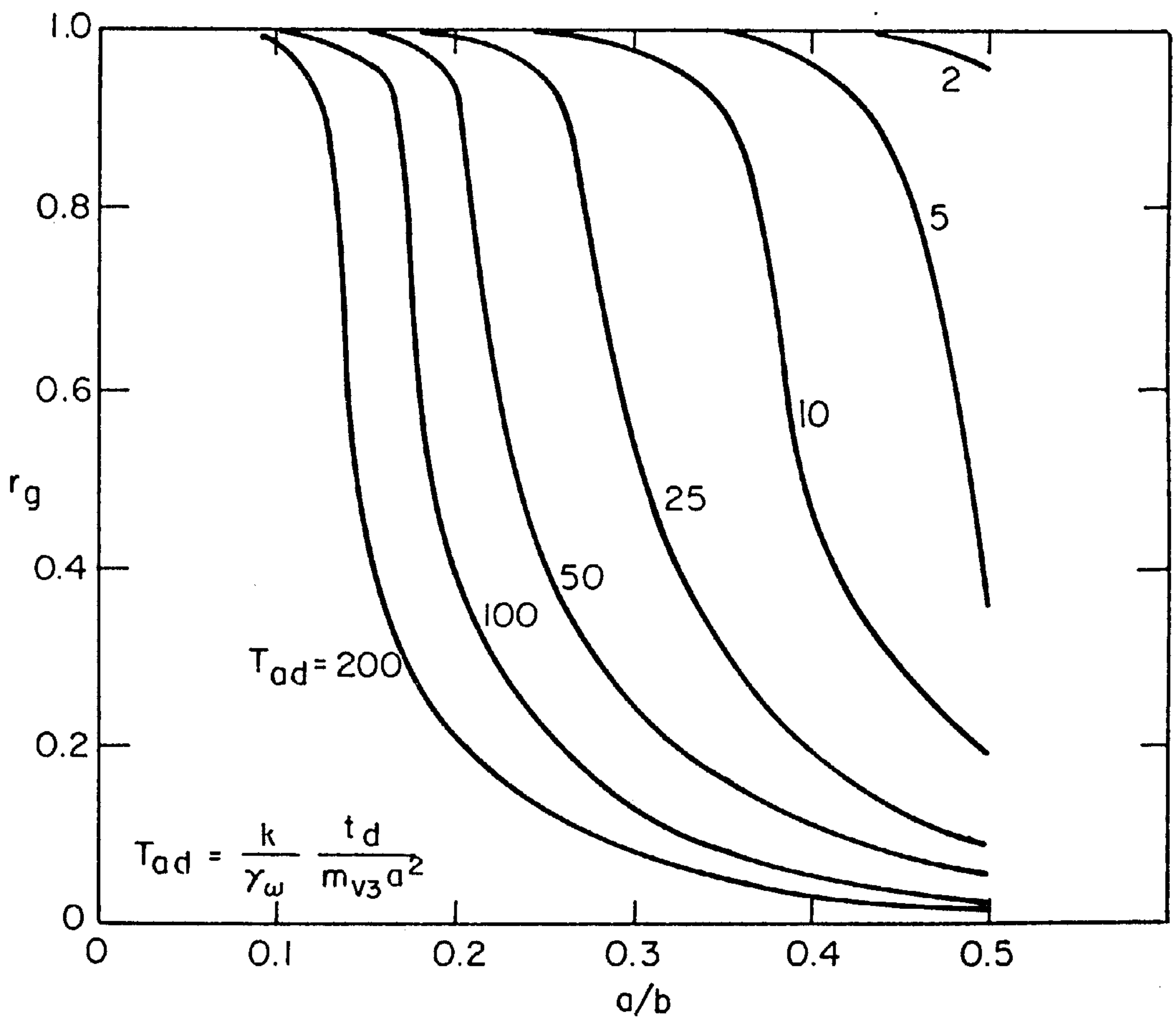

Fig. 9 RELATIONSHIP BETWEEN GREATEST PORE PRESSURE RATIO AND DRAIN SYSTEM PARAMETERS FOR $N_{eq}/N_\ell = 4$

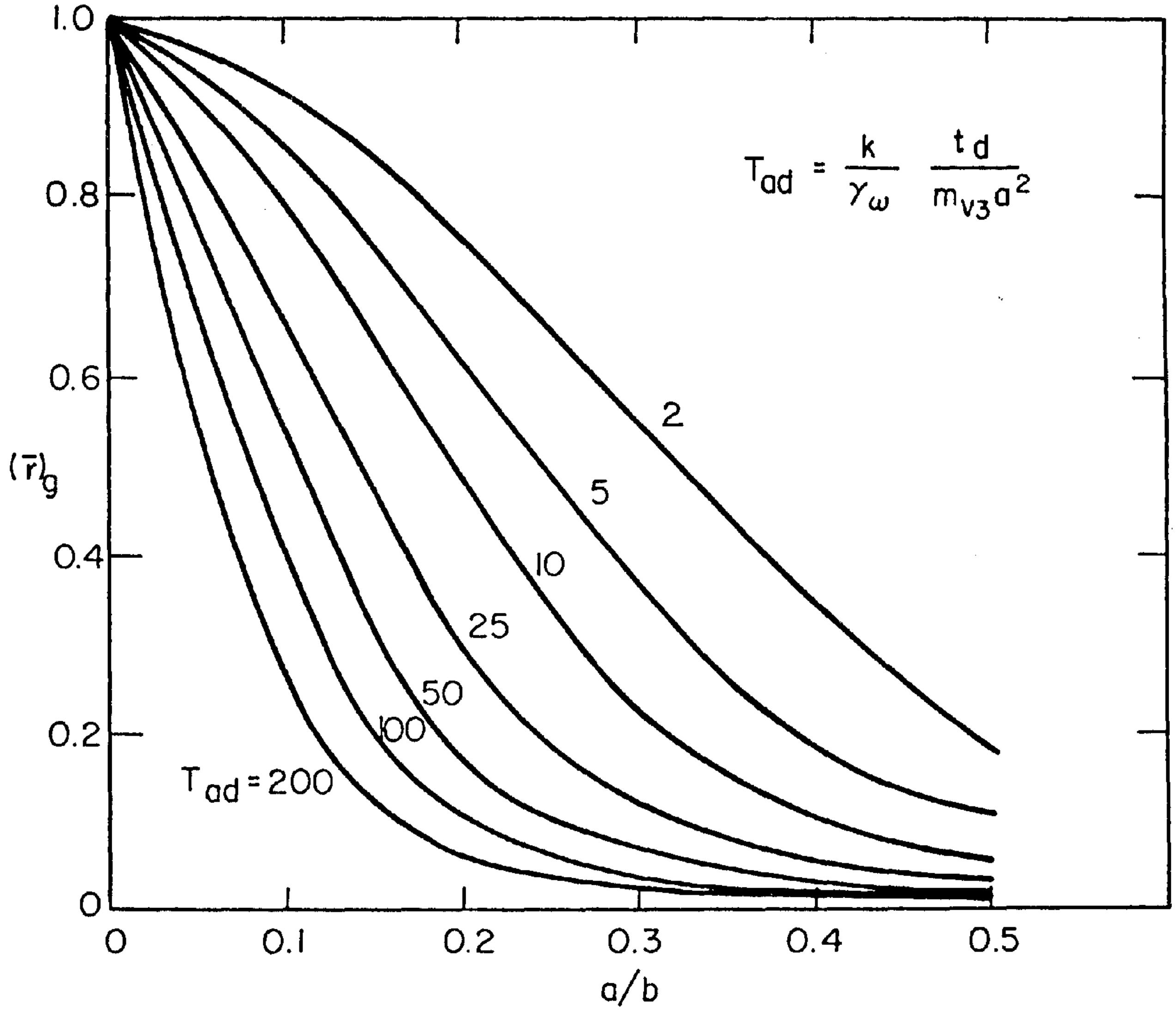

Fig. 10 RELATIONSHIP BETWEEN GREATEST AVERAGE PORE PRESSURE RATIO AND DRAIN SYSTEM PARAMETERS FOR $N_{eq}/N_\ell = 1$

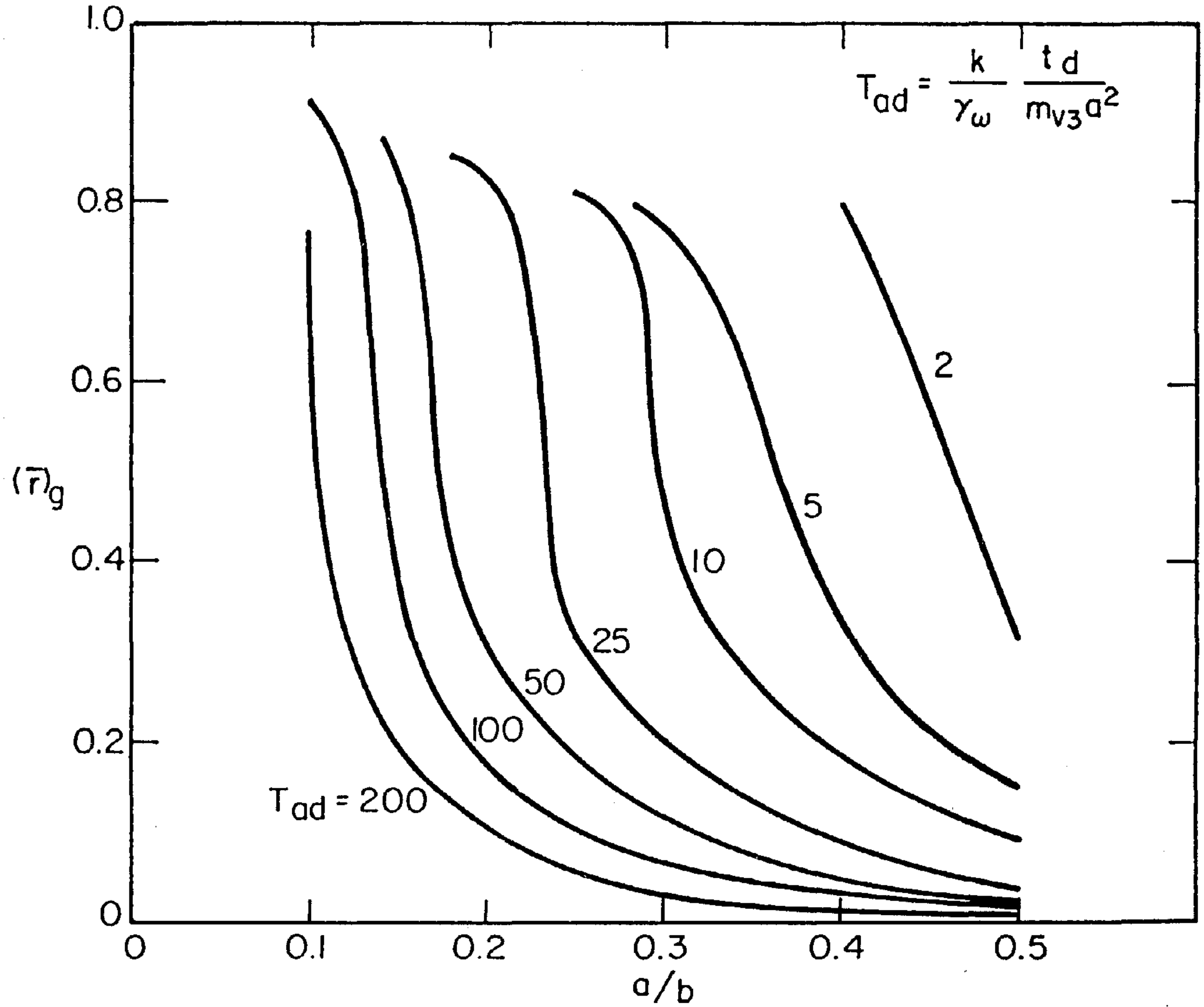

Fig. 11 RELATIONSHIP BETWEEN GREATEST AVERAGE PORE PRESSURE RATIO AND DRAIN SYSTEM PARAMETERS FOR $N_{eq}/N_\ell = 2$

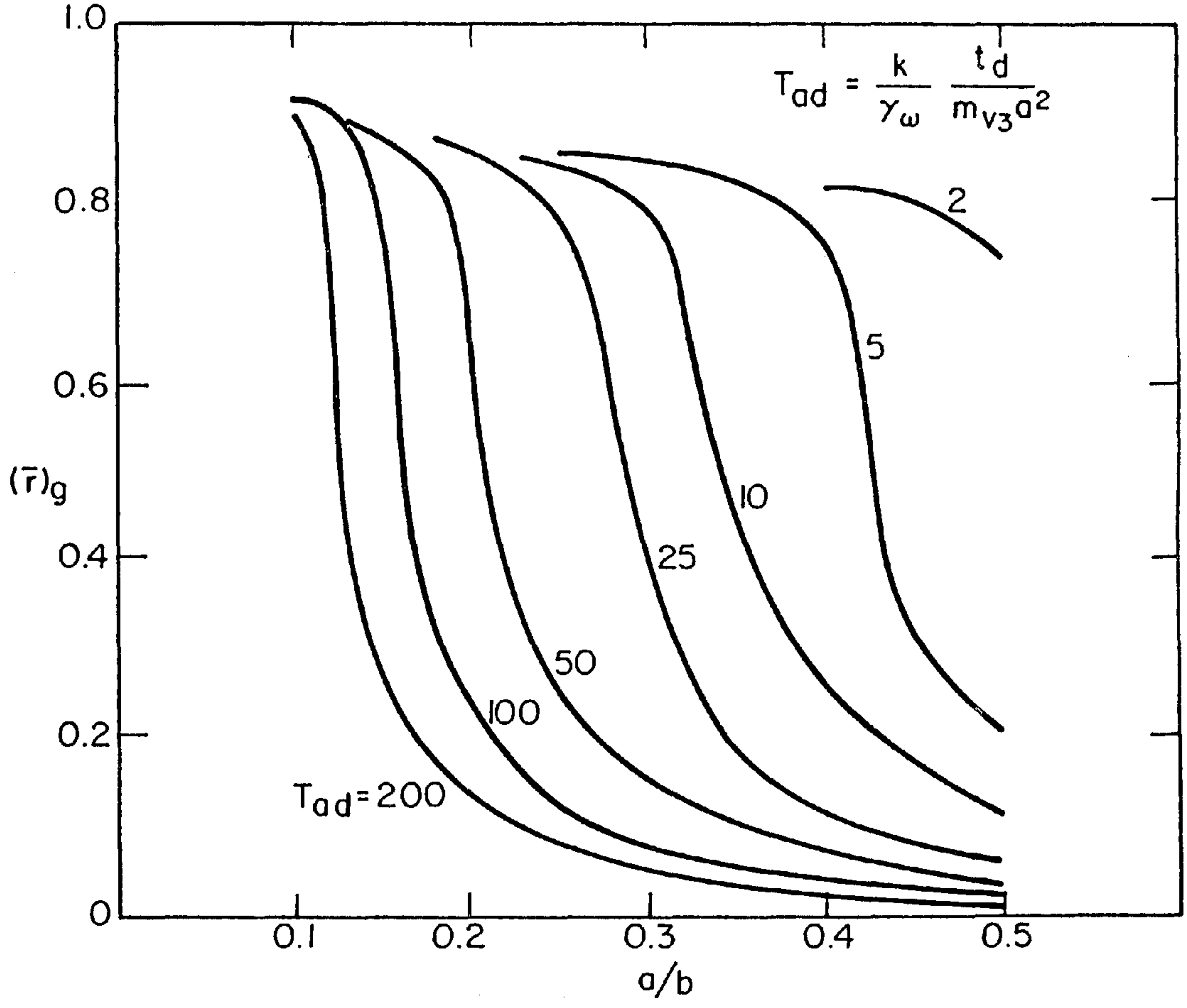

Fig. 12 RELATIONSHIP BETWEEN GREATEST AVERAGE PORE PRESSURE RATIO AND DRAIN SYSTEM PARAMETERS FOR $N_{eq}/N_{\ell} = 3$

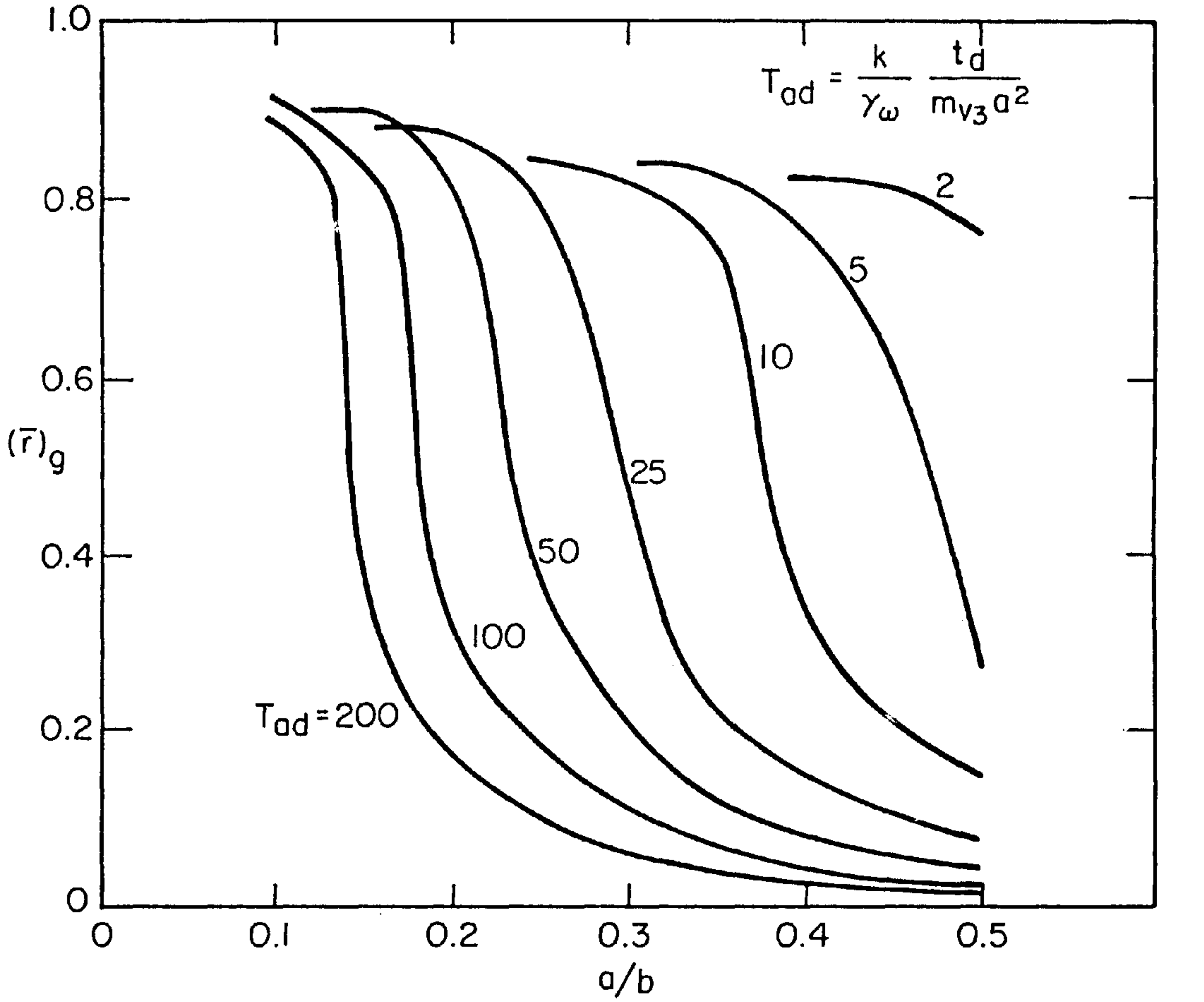

Fig. 13 RELATIONSHIP BETWEEN GREATEST AVERAGE PORE PRESSURE RATIO AND DRAIN SYSTEM PARAMETERS FOR $N_{eq}/N_\ell = 4$

so that a spacing of 8 ft would have to be adopted. A comparison with Fig. 11 shows that a similar spacing would have been adopted if a greatest average pore pressure ratio $(\bar{r})_g = 0.6$ had been considered allowable.

EFFECT OF PERMEABILITY OF FILLING MATERIAL

In the calculation of the previous results it has been assumed that the material within the gravel drain was infinitely permeable. The effect of this assumption can be examined by assuming a finite permeability for this material and again solving Eqn. 5. To simplify the analysis it has been assumed that radial drainage also occurs in the filling material but there is an infinitely pervious pipe at its center. (If no such pipe were present the generated excess pore water pressures within the drain-layer system would redistribute because of their different properties and then dissipate to a final non-zero value, since no pore water could escape.) To illustrate the effect, the case of a sand deposit with $N_{eq}/N_\ell = 2$ and $T_{bd} = 1.25$ with a spacing ratio $a/b = 0.2$ was analyzed for a range of values of k_f/k where k_f denotes the permeability of the filling material. For the sake of simplicity it was assumed that the filling material had the same liquefaction characteristics as the sand. The results of the analysis are shown in Fig. 14 and it can be seen that the drain operates perfectly provided it has a permeability of the order of 200 times that of the sand. Thus it would appear that for most sands, medium to fine gravels would provide adequate filling material for the drains.

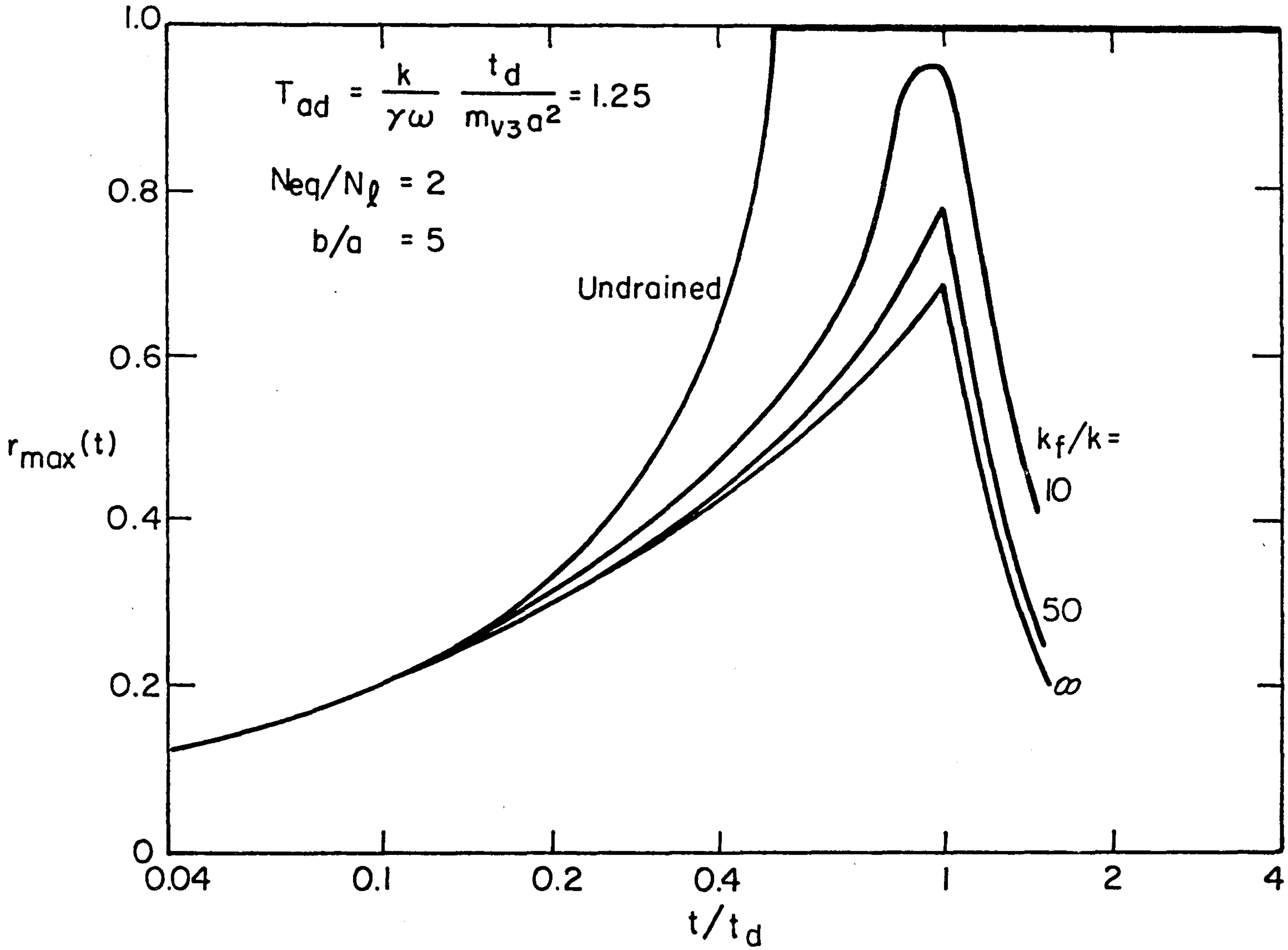

Fig. 14 EFFECT OF PERMEABILITY OF DRAIN MATERIAL ON RATE OF PORE PRESSURE DISSIPATION

EFFECT OF VERTICAL DRAINAGE

The preceding analyses have been based on the assumption that vertical drainage played an insignificant role in the functioning of the drains. To illustrate this effect, consider the case of a 20 ft layer of the material described in the previous example resting on an impermeable layer and buried beneath a pervious fill 50 ft deep, both materials having a unit weight of 120 lbs/ft^3. Suppose also that the vertical permeability of the sand is one third of its horizontal permeability.

It was assumed that 8" diameter sand drains were placed in this material at an effective spacing of 6 ft. The problem was analyzed first assuming that only radial drainage could occur and that the soil had a uniform initial effective stress equal to that at its midsection, and secondly allowing the initial effective stress to vary throughout the layer and allowing both vertical and horizontal drainage to occur. The results of these analyses are compared in Fig. 15, and are virtually indistinguishable within the accuracy of plotting.

Of course there may be many situations in which vertical drainage may have a significant effect but it is conjectured that for many of these cases it will be sufficiently accurate to use the relationship:

$$\begin{array}{l} \text{Greatest pore} \\ \text{pressure ratio} \\ \text{developed} \end{array} \simeq \begin{array}{l} \text{Greatest pore pressure} \\ \text{ratio for purely radial} \\ \text{drainage of midsection} \end{array} \times \begin{array}{l} \text{Degree of consolidation} \\ \text{for purely vertical} \\ \text{drainage of the layer} \end{array}$$

Thus the data in Figs. 6 to 13 could still be used to evaluate the efficiency of any proposed drainage system.

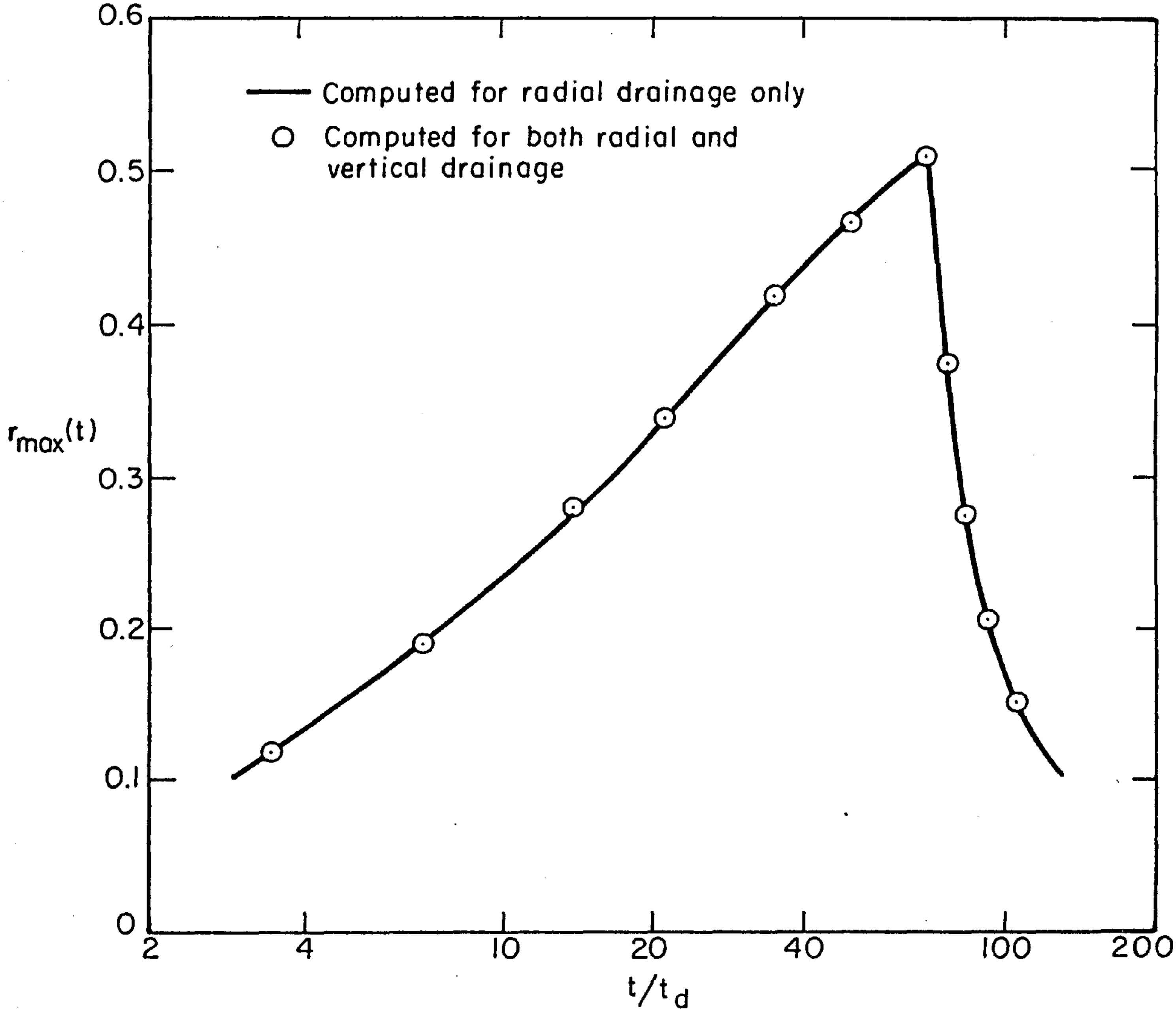

Fig. 15 EFFECT OF COMBINED RADIAL AND VERTICAL DRAINAGE ON MAXIMUM PORE PRESSURE RATIO

CONCLUSION

In many cases, the installation of a drainage system as described in the preceding pages offers an attractive and economical procedure for stabilizing an otherwise potentially liquefiable sand deposit. In fact, the method has already been used in one case involving the construction of stone columns in a relatively loose sand deposit and it is currently being proposed for stabilization of a medium dense sand layer which is known to have developed some degree of liquefaction in a recent earthquake but which appears to be too dense for stabilization by further densification using currently available procedures.

The simplified theory presented in the preceding pages provides a convenient basis for evaluating the possible effectiveness of a gravel drain system in such cases. Where appropriate, additional analyses may readily be made using the computer program LARF but for most practical cases, it is believed that the results presented in Figs. 6 to 13 will provide an adequate basis for design and selection of a suitable drain system for effective stabilization of a potentially liquefiable sand deposit.

ACKNOWLEDGEMENTS

The studies described in the previous pages were supported by Grant N. ENV75-21875 from the National Science Foundation and by a grant from the Australian-American Education Foundation. The support of these agencies is gratefully acknowledged.

REFERENCES

(1) Ambraseys, N. and Sarma, S. (1969) "Liquefaction of Soil Induced by Earthquakes," Bull. Seis. Soc. of America, Vol. 59, No. 2, 1969, pp. 651-664.

(2) DeAlba, Pedro, Chan, Clarence K. and Seed, H. Bolton (1975) "Determination of Soil Liquefaction Characteristics by Large Scale Laboratory Tests," Earthquake Engineering Research Center, Report No. EERC 75-14, May 1975.

(3) Lee, Kenneth L. and Albaiso, Aurelio (1974) "Earthquake Induced Settlements in Saturated Sands," Journal of the Geotechnical Engineering Division, ASCE, Vol. 100, No. GT4, Proc. Paper 10496, April 1974, pp. 387-406.

(4) Seed, H. B. and Idriss, I. M. (1967) "Analysis of Soil Liquefaction: Niigata Earthquake," Journal of the Soil Mechanics and Foundations Division, ASCE, Vol. 93, No. SM3, Proc. Paper 5233, May 1967, pp. 83-108.

(5) Seed, H. B. and Idriss, I. M. (1971) "Simplified Procedure for Evaluating Soil Liquefaction Potential," Journal of the Soil Mechanics and Foundations Division, ASCE, Vol. 97, No. SM9, Proc. Paper 8371, September 1971, pp. 1249-1273.

(6) Seed, H. B. Idriss, I. M., Makdisi, F., and Bannerjee, N. (1975) "Representation of Irregular Stress Time Histories by Equivalent Uniform Stress Series in Liquefaction Analyses," Earthquake Engineering Research Center, Report No. EERC 75-29, October.

(7) Seed, H. B. and Lee, K. L. (1966) "Liquefaction of Saturated Sands during Cyclic Loading," Journal of the Soil Mechanics and Foundations Division, ASCE, Vol. 92, No. SM6, Proc. Paper 4973, November, 1966, pp. 105-134.

(8) Seed, H. B., Martin, P. P. and Lysmer, J. (1975) "The Generation and Dissipation of Pore Water Pressures During Soil Liquefaction," Earthquake Engineering Research Center, Report No. EERC 75-26, August 1975.

(9) Wong, Robert T., Seed, H. Bolton and Chan, Clarence K. (1975) "Cyclic Loading Liquefaction of Gravelly Soils," Journal of the Geotechnical Engineering Division, ASCE, Vol. 101, No. GT6, Proc. Paper 11396, June.

(10) Yoshimi, Yoshiaki and Kuwabara, Fumio (1973) "Effects of Subsurface Liquefaction on the Strength of Surface Soil," Soils and Foundations, Japanese Society of Soil Mechanics and Foundation Engineering, Vol. 19, No. 2, June 1973, pp. 67-81.

(11) Zienkiewicz, O. C. (1971) "The Finite Element Method in Engineering Science," McGraw-Hill.

NOTATION

$2a$	Diameter of sand drain.
$2b$	Effective spacing of sand drains.
dt	Increment of time.
k	Isotropic permeability.
k_h	Horizontal permeability.
k_v	Vertical permeability.
m_{v3}	Coefficient of volume decrease.
N	Number of cycles.
N_{eq}	Number of uniform stress cycles equivalent to the earthquake.
N_e	Number of cycles to liquefaction.
r_u	Pore pressure ratio.
$r_{max}(t)$	Maximum pore pressure ratio at time t.
(r_g)	Greatest average pore pressure ratio.
t	Time.
t_d	Duration of the earthquake.
t_u	Time at which liquefaction occurs under undrained conditions.
T_{ad}	Dimensionless time factor.
T_{bd}	Dimensionless time factor.
α	Parameter describing pore pressure generation in sand.
ε	Volume strain.
γ_ω	Unit weight of water.
σ'_o	Initial mean bulk, or vertical, effective stress.

APPENDIX A

A computer program LARF, Liquefaction Analysis for Radial Flow, has been written to integrate Eqn. 6 numerically using the finite element approach. The program consists of a main program LARF and 6 subroutines DATA, STIFF, DGNL, SETUP, DUG, SYMSOL. The action of the program is shown schematically in the flow chart, Fig. 16. The finite element discretisation for such problems is well known (see Zienkiewicz, 1971) and so is not detailed here; details of the numerical determination of the source function $\partial u_g/\partial t$ have been given by Seed et. al. (1975).

Input Details

Data for the program LARF must be input as described in Table 1 and read by means of the subroutine DATA. An illustrative example is given later. The data may be in any set of consistent units.

Output Details

The output of program LARF consists of the values of the maximum pore pressure ratio, average pore pressure ratio and greatest pore pressure ratio as well as the values of the excess pore pressures at all the node points.

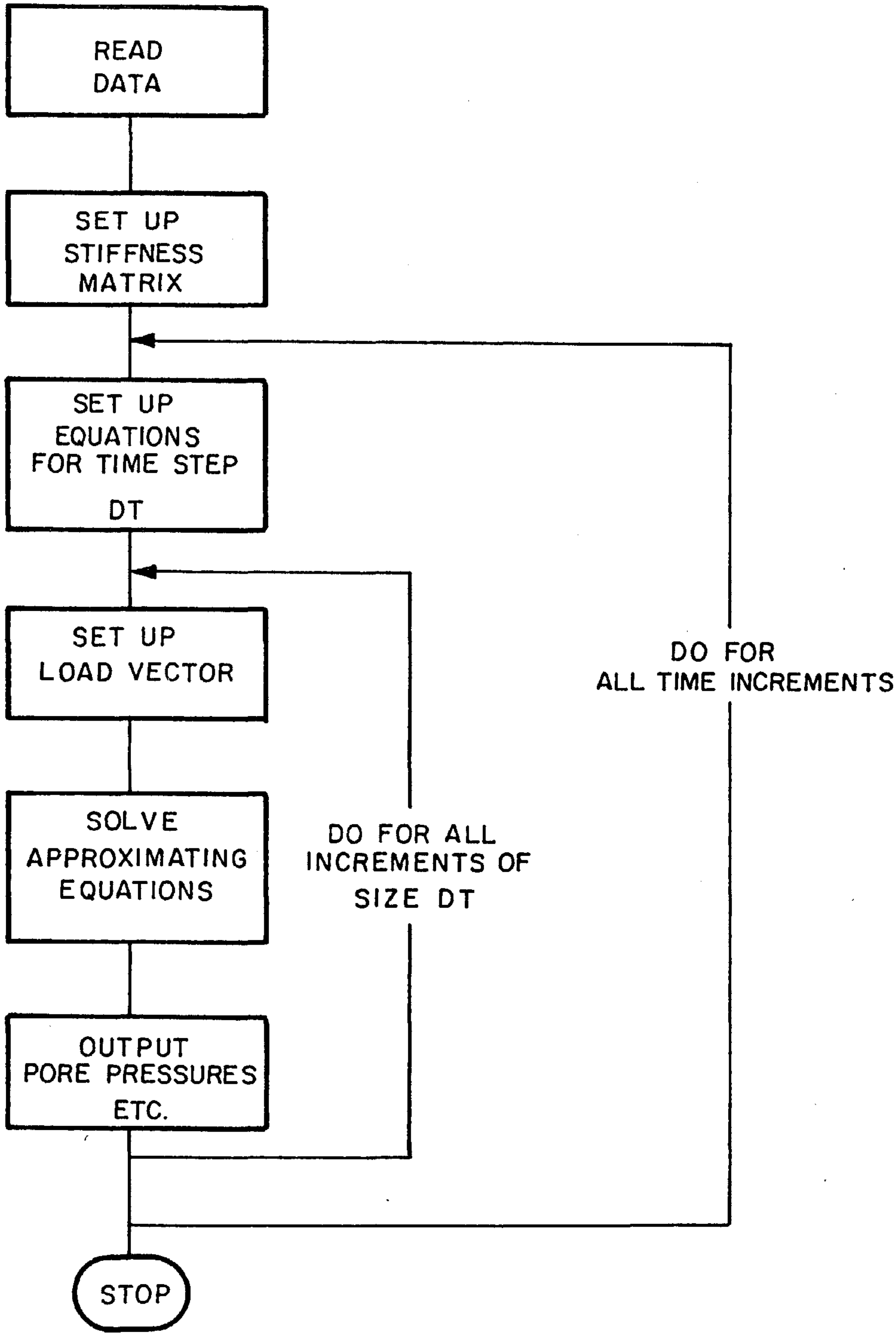

Fig. 16 FLOW CHART FOR LARF

TABLE 1

SEQUENCE FOR READING DATA

	No. of DATA CARDS	DESCRIPTION	FORMAT
1.	1	Read unit weight of water GAMAW.	F10.4
2.	1	Read duration of earthquake TD.	F10.4
3.	1	Read initial vertical effective stress ESV.	F10.4
4.	1	Read the number of nodes NR.	I4
5.	NR	Read the node number (J), R coordinate R(J), number of equivalent cycles ENE(J), and number of cycles to liquefaction ENL(J) for each node.	I4,3F10.4
6.	1	Read number of different time steps, NINT.	I4
7.	NINT	Read number of time steps NDELT(I), and magnitude of that time step DELT(I)	I4,F10.4
8.	NR-1	Read element number JR, horizontal permeability of the element PERMR(JR) and compressibility of the element COMX(JR)	I4,2E12.6

Special Details

At the moment the program is set up to cope with

(a) A maximum number of 50 nodes NRA

(b) A maximum number of 10 different time increments NINTA.

If desired, this can be changed by altering the statements

NRA = 50	to say	NRA = 100
NINTA = 10	to say	NINTA = 20

and the replacement, in the common blocks and dimension statements, of

50	by	100
49	by	99
10	by	20

The finite element nodes should be numbered from the drain outwards. It will always be assumed that the innermost node is free to drain and thus has no excess pore pressure and that the outer-most node lies on an impermeable boundary. The elements are bounded by pairs of adjacent nodes and are numbered from the inner-most to the outer-most.

Example

To illustrate the use of LARF, consider the drain system discussed in the earlier example. Suppose, in the finite element discretisation, that 7 equally-spaced nodes are chosen and that the solution is calculated at 30 distinct times, the first 20 at 3.5 second intervals, the subsequent 10 at five second intervals. Force, distance and time will be expressed in terms of k Newtons, meters and seconds respectively.

It will be assumed for definiteness that the initial effective stress has a value of 100 units although it should be noted that the pore pressure ratios are independent of this value.

The above problem should be regarded merely as illustrative. In any practical situation, the error due to choice of time step should be reduced to an acceptable level by an independent study (series of trial runs) examining the effect of changing the step size.

LISTING AND SAMPLE DATA FOR PROGRAM LARF

```
      PROGRAM  LARF(INPUT,OUTPUT)
      COMMON/NDATA/NR,NRA,R(50),ESV,N,M
      COMMON/TDATA/NINT,NINTA,DELT(10),NDELT(10)
      COMMON/EDATA/MR,MRA,PERMR(49),COMX(49),GAMAW
      COMMON/EQD/ENE(50),ENL(50),TD
      DIMENSION AA(50,2),AAQ(50,2),DIAG(50,2)
      DIMENSION U(50),BQ(50),UGT(50)
      NRA=50
      NINTA=10
      MRA=NRA-1
      NA=NRA
      MA=2
C
C     READ INPUT DATA
C
      CALL DATA
      ICH=1
      IF(N.GT.NA) GOTO 19
      ICH=2
      IF(M.GT.MA) GOTO19
C
C     SET UP STIFFNESS MATRIX
C
      CALL STIFF(AA,NA,MA)
C
C     INITIALISE PORE PRESSURES
C
      DO 210 I=1,N
      U(I)=0.0
  210 CONTINUE
      T=0.0
      RGREAT=0.0
      DO 200 JT=1,NINT
      DT=DELT(JT)
      NT=NDELT(JT)
      KKK=1
C
C     SET UP APPROXIMATING EQUATIONS
C
      CALL SETUP(ALPHA,DT,AA,DIAG,U,AAQ,NA,MA)
      DO 200 IT=1,NT
      T=T+DT
C
C     CALCULATE LOAD VECTOR
C
      CALL LVECT(ALPHA,DT,T,AA,DIAG,U,UGT,BQ,NA,MA)
C
C     SOLVE APPROXIMATING EQUATIONS
C
      CALL SYMSOL(AAQ,BQ,N,M,NA,MA,KKK)
      KKK=2
C
C     CALCULATE MAXIMUM,AVERAGE AND GREATEST PORE PRESSURE RATIOS
C
      RMAX=0.0
      DO 10 I=1,N
      U(I)=BQ(I)
      AR=U(I)/ESV
      IF(AR.GT.RMAX) RMAX=AR
   10 CONTINUE
      IF(RMAX.GT.RGREAT) RGREAT=RMAX
      AREA=0.0
      SUM=0.0
```

```
      DO 15 J=2,N
      QUANT=0.5*(R(J)+R(J-1))*(R(J)-R(J-1))
      AREA=AREA+QUANT
   15 SUM=SUM+0.5*(U(J)+U(J-1))*QUANT
      UAV=SUM/AREA/ESV
C
C     OUTPUT PORE PRESSURE RATIOS
C
      PRINT 93,T,RMAX,UAV,RGREAT
   93 FORMAT(///26X,*TIME = *,F10.4/
     2*  MAXIMUM  PORE PRESSURE RATIO = *,F10.4/
     1*  AVERAGE  PORE PRESSURE RATIO = *,F10.4/
     3*  GREATEST PORE PRESSURE RATIO = *,F10.4//)
      PRINT 94
   94 FORMAT(*  EXCESS PORE WATER PRESSURE(I)*//)
      PRINT 95,((I,U(I)),I=1,N)
   95 FORMAT(5(2X,I4,F10.4))
  200 CONTINUE
      GOTO 39
C
C     DIAGNOSTICS FOR LARF
C
   19 CONTINUE
      PRINT 29,ICH
   29 FORMAT(*DIAGNOSTICS FOR STILL ICH=*,I4)
   39 CONTINUE
      END
      SUBROUTINE DATA
      COMMON/NDATA/NR,NRA,R(50),ESV,N,M
      COMMON/TDATA/NINT,NINTA,DELT(10),NDELT(10)
      COMMON/EDATA/MR,MRA,PERMR(49),COMX(49),GAMAW
      COMMON/EQD/ENE(50),ENL(50),TD
C
C     READ DATA
C
C
C     READ THE UNIT WEIGHT OF WATER
C
      READ 71,GAMAW
   71 FORMAT(8F10.4)
      PRINT 106,GAMAW
  106 FORMAT(//*  UNIT WEIGHT OF WATER     = *,F10.4//)
C
C     READ DURATION OF THE EARTHQUAKE
C
  107 FORMAT(//*  DURATION OF EARTHQUAKE  = *,F10.4//)
      READ 71,TD
      PRINT 107,TD
C
C     READ THE INITIAL VERTICAL STRESS
C
      READ 71,ESV
      PRINT 103,ESV
  103 FORMAT(//* INITIAL EFFECTIVE STRESS =*,F10.4//)
C
C     READ THE NUMBER OF NODES
C
      READ 1,NR
      PRINT 101,NR
  101 FORMAT(//* NUMBER OF NODES =*,I4//)
      ICH=1
      IF(NR.GT.NRA) GOTO 19
      MR=NR-1
```

```
      N=NR
      ICH=2
      M=2
C
C     READ THE NODAL DATA
C
      PRINT 102
  102 FORMAT(//*   NODE    R COORDINATE     EQUIVALENT      NUMBER*
     1* OF CYCLES*
     1 /*  NUMBER *,16X,*NUMBER OF CYCLES   TO LIQUEFACTION*//)
      DO 66 I=1,NR
      READ 72,J,R(J),ENE(J),ENL(J)
      PRINT 73,J,R(J),ENE(J),ENL(J)
   72 FORMAT(I4,3F10.4)
   73 FORMAT(3X,I4,5X,F10.4,6X,F10.4,8X,F10.4)
   66 CONTINUE
C
C     READ TIME STEP DATA
C
      READ 1,NINT
      PRINT 115,NINT
  115 FORMAT(//* NUMBER OF DIFFERENT TIME STEPS =*,I4//)
      ICH=4
      IF(NINT.GT.NINTA) GOTO 19
      DO 17 I=1,NINT
      READ 5,NDELT(I),DELT(I)
    5 FORMAT(I4,F10.4)
      PRINT 117,NDELT(I),DELT(I)
  117 FORMAT(* NUMBER OF STEPS = *,I4,* TIME INCREMENT=*,F10.4)
   17 CONTINUE
C
C
C     READ THE ELEMENT DATA
C
      PRINT 105
  105 FORMAT(//*  ELEMENT NUMBER PERMEABILITY COMPRESSIBILITY*//)
      DO 15 JR=1,MR
      READ 79,I,PERMR(I),COMX(I)
   79 FORMAT(I4,2E12.5)
      PRINT 104 ,JR,PERMR(JR),COMX(JR)
  104 FORMAT(8X,I4,5X,E12.5,4X,E12.5)
   15 CONTINUE
   10 CONTINUE
    1 FORMAT(2I4)
      RETURN
   19 CONTINUE
      PRINT 29,ICH
   29 FORMAT(* DIAGNOSTIC SUBROUTINE DATA ICH =*,I4)
      END
      SUBROUTINE STIFF(AA,NA,MA)
      COMMON/NDATA/NR,NRA,R(50),ESV,N,M
      COMMON/EDATA/MR,MRA,PERMR(49),COMX(49),GAMAW
      DIMENSION AA(NA,MA)
C
C      SET UP STIFFNESS MATRIX A
C
      DO 16 I=1,N
      DO 16 J=1,M
   16 AA(I,J)=0.0
      DO 40 JR=1,MR
      DR=R(JR+1)-R(JR)
      RBAR=R(JR)+0.5*DR
      AH=PERMR(JR)*RBAR/DR/GAMAW
```

```
      IA=JR
      IB=IA+1
      AA(IA,1)=AA(IA,1)+AH
      AA(IA,2)=AA(IA,2)-AH
      AA(IB,1)=AA(IB,1)+AH
   40 CONTINUE
      RETURN
      END
C
C     CALCULATE THE LOAD VECTOR
C
      SUBROUTINE LVECT(ALPHA,DT,T,AA,DIAG,U,UGT,BQ,NA,MA)
      COMMON/NDATA/NR,NRA,R(50),ESV,N,M
      COMMON/TDATA/NINT,NINTA,DELT(10),NDELT(10)
      COMMON/EDATA/MR,MRA,PERMR(49),COMX(49),GAMAW
      COMMON/EQD/ENE(50),ENL(50),TD
      DIMENSION AA(NA,MA),BQ(NA),U(NA)
      DIMENSION UGT(NA),DIAG(NA,MA)
      EPS=0.01
      ES0=ESV
      DO 240 K=1,NR
      ES=ES0-U(K)
      IF(ES.LT.EPS) U(K)=ES0
      UAV=U(K)
      CALL DUG(ENE(K),ENL(K),TD,UAV,ESV,T,DT,UGH)
      UGT(K)=UGH
      IF(ES.LT.EPS) UGT(K)=0.0
  240 CONTINUE
      DO 300 I=1,N
      IM=I-1
      SUN=0.0
      DUN=0.0
      LIM=I+1-M
      IF(LIM.LT.1) LIM=1
      IF(LIM.GT.IM) GOTO 777
      DO 330 K=LIM,IM
      DUN=DUN+DIAG(K,I-K+1)*(U(K)+UGT(K))
  330 SUN=SUN+AA(K,I-K+1)*U(K)
  777 CONTINUE
      LIM=M+I-1
      IF(LIM.GT.N) LIM=N
      DO 320 K=I,LIM
      DUN=DUN+DIAG(I,K-I+1)*(U(K)+UGT(K))
  320 SUN=SUN+AA(I,K-I+1)*U(K)
  300 BQ(I)=DUN-SUN*DT*ALPHA
      BQ(1)=0.0
      RETURN
      END
      SUBROUTINE DGNL(DIAG,U,NA,MA)
      COMMON/NDATA/NR,NRA,R(50),ESV,N,M
      COMMON/EDATA/MR,MRA,PERMR(49),COMX(49),GAMAW
      DIMENSION DIAG(NA,MA)
      DIMENSION U(NA)
      DO 15 I=1,N
      DO 15 J=1,M
   15 DIAG(I,J)=0.0
      DO 220 JR=1,MR
      DR=R(JR+1)-R(JR)
      RBAR=R(JR)+0.5*DR
      IA=JR
      IB=IA+1
      QUANT=0.5*COMX(JR)*DR*RBAR
      DIAG(IA,1)=DIAG(IA,1)+QUANT
```

```
      DIAG(IB,1)=DIAG(IB,1)+QUANT
  220 CONTINUE
      RETURN
      END
      SUBROUTINE SETUP(ALPHA,DT,AA,DIAG,U,AAQ,NA,MA)
      COMMON/NDATA/NR,NRA,R(50),ESV,N,M
      COMMON/EQD/ENE(50),ENL(50),TD
      DIMENSION AA(NA,MA),AAQ(NA,MA),DIAG(NA,MA)
      DIMENSION U(NA)
C
C     SET UP APPROXIMATING EQUATIONS
C
      ALPHA=0.5
      CALL DGNL(DIAG,U,NA,MA)
      BETA=1.0-ALPHA
      DO 350 I=1,N
      DO 360 J=1,M
  360 AAQ(I,J)=AA(I,J)*DT*BETA+DIAG(I,J)
  350 CONTINUE
      K=1
      DO 430 J=1,M
      L=K-J+1
      IF(L.GT.0) AAQ(L,J)=0.0
  430 AAQ(K,J)=0.0
      AAQ(K,1)=1.0
      RETURN
      END
      SUBROUTINE DUG(ENE,ENL,TD,U,ESV,TT,DT,UGH)
C
C     CALCULATE SOURCE TERM
C
      UGH=0.0
      IF(TT.GT.TD) GOTO 25
      ALPHA=0.7
      BETA=1.0/ALPHA
      PI=3.14159265
      XX=1.0
      RU=U/ESV
      ARG=0.5*(1.0-COS(PI*RU))
      RN0=ARG**ALPHA
      DR=DT/TD*ENE/ENL
      RN1=RN0+DR
      ARG=2.0*RN1**BETA-1.0
      IF(ARG.GT.XX) ARG=XX
      RU=0.5+ASIN(ARG)/PI
      UGH=RU*ESV-U
   25 CONTINUE
      RETURN
      END
      SUBROUTINE SYMSOL(A,B,NN,MM,NA,MA,KKK)
      DIMENSION A(NA,MA),B(NA)
C
C     SOLVE SIMULTANEOUS EQUATIONS
C
      EPS=0.000001
      ICH=1
      IF(NN.GT.NA) GOTO 19
      ICH=2
      IF(MM.GT.MA) GOTO 19
      IF(KKK.GT.1) GOTO 2000
 1000 DO 280 N=1,NN
      DO 260 L=2,MM
      ICH=3
```

```
      IF(ABS(A(N,1)).LT.EPS) GOTO 19
      C=A(N,L)/A(N,1)
      I=N+L-1
      IF(NN-I) 260,240,240
  240 J=0
      DO 250 K=L,MM
      J=J+1
  250 A(I,J)=A(I,J)-C*A(N,K)
  260 A(N,L)=C
  280 CONTINUE
 2000 DO 290 N=1,NN
      DO 285 L=2,MM
      I=N+L-1
      IF(NN-I) 290,285,285
  285 B(I)=B(I)-A(N,L)*B(N)
  290 B(N)=B(N)/A(N,1)
      N=NN
  300 N=N-1
      IF(N) 350,500,350
  350 DO 400 K=2,MM
      L=N+K-1
      IF(NN-L) 400,370,370
  370 B(N)=B(N)-A(N,K)*B(L)
  400 CONTINUE
      GOTO 300
  500 RETURN
   19 CONTINUE
      PRINT 29,ICH
   29 FORMAT(*DIAGNOSTICS FOR SYMSOL*,I4)
      END

9.8
70.0
100.0
    7
    1  0.3050  24.0        12.0
    2  0.4575  24.0        12.0
    3  0.6100  24.0        12.0
    4  0.7625  24.0        12.0
    5  0.9150  24.0        12.0
    6  1.0675  24.0        12.0
    7  1.2200  24.0        12.0
    2
   20  3.5
   10  5.0
    1+0.10000E-04+0.42000E-04
    2+0.10000E-04+0.42000E-04
    3+0.10000E-04+0.42000E-04
    4+0.10000E-04+0.42000E-04
    5+0.10000E-04+0.42000E-04
    6+0.10000E-04+0.42000E-04


**END OUTPUT
**END OUTPUT
```

SAMPLE OF OUTPUT FROM PROGRAM LARF

```
UNIT WEIGHT OF WATER     =     9.8000

DURATION OF EARTHQUAKE   =    70.0000

INITIAL EFFECTIVE STRESS =   100.0000

NUMBER OF NODES =    7
```

NODE NUMBER	R COORDINATE	EQUIVALENT NUMBER OF CYCLES	NUMBER OF CYCLES TO LIQUEFACTION
1	.3050	24.0000	12.0000
2	.4575	24.0000	12.0000
3	.6100	24.0000	12.0000
4	.7625	24.0000	12.0000
5	.9150	24.0000	12.0000
6	1.0675	24.0000	12.0000
7	1.2200	24.0000	12.0000

NUMBER OF DIFFERENT TIME STEPS = 2

NUMBER OF STEPS = 20 TIME INCREMENT= 3.5000
NUMBER OF STEPS = 10 TIME INCREMENT= 5.0000

ELEMENT NUMBER	PERMEABILITY	COMPRESSIBILITY
1	.10000E-04	.42000E-04
2	.10000E-04	.42000E-04
3	.10000E-04	.42000E-04
4	.10000E-04	.42000E-04
5	.10000E-04	.42000E-04
6	.10000E-04	.42000E-04

TIME = 3.5000
MAXIMUM PORE PRESSURE RATIO = .1213
AVERAGE PORE PRESSURE RATIO = .1074
GREATEST PORE PRESSURE RATIO = .1218

EXCESS PORE WATER PRESSURE(I)

1	0.	2	7.3377	3	10.2200	4	11.4170	5	11.9231
6	12.1262	7	12.1783						

TIME = 7.0000
MAXIMUM PORE PRESSURE RATIO = .1946
AVERAGE PORE PRESSURE RATIO = .1626
GREATEST PORE PRESSURE RATIO = .1946

EXCESS PORE WATER PRESSURE(I)

1	0.	2	8.9481	3	14.1674	4	17.0520	5	18.5596
6	19.2612	7	19.4558						

```
                         TIME =      10.5000
MAXIMUM  PORE PRESSURE RATIO =        .2489
AVERAGE  PORE PRESSURE RATIO =        .2051
GREATEST PORE PRESSURE RATIO =        .2489

EXCESS PORE WATER PRESSURE(I)

    1    0.          2    11.2629     3    17.4549     4    21.2029     5    23.4170
    6   24.5583      7    24.8932


                         TIME =      14.0000
MAXIMUM  PORE PRESSURE RATIO =        .2920
AVERAGE  PORE PRESSURE RATIO =        .2389
GREATEST PORE PRESSURE RATIO =        .2920

EXCESS PORE WATER PRESSURE(I)

    1    0.          2    12.5708     3    20.1118     4    24.6700     5    27.3695
    6   28.7813      7    29.2007


                         TIME =      17.5000
MAXIMUM  PORE PRESSURE RATIO =        .3280
AVERAGE  PORE PRESSURE RATIO =        .2670
GREATEST PORE PRESSURE RATIO =        .3280

EXCESS PORE WATER PRESSURE(I)

    1    0.          2    13.9745     3    22.2455     4    27.4612     5    30.6286
    6   32.2993      7    32.7966


                         TIME =      21.0000
MAXIMUM  PORE PRESSURE RATIO =        .3583
AVERAGE  PORE PRESSURE RATIO =        .2907
GREATEST PORE PRESSURE RATIO =        .3583

EXCESS PORE WATER PRESSURE(I)

    1    0.          2    14.9659     3    24.1157     4    29.8624     5    33.3855
    6   35.2689      7    35.8341


                         TIME =      24.5000
MAXIMUM  PORE PRESSURE RATIO =        .3845
AVERAGE  PORE PRESSURE RATIO =        .3112
GREATEST PORE PRESSURE RATIO =        .3845

EXCESS PORE WATER PRESSURE(I)
```

1	0.	2	15.9430	3	25.6709	4	31.9117	5	35.7654
6	37.8296	7	38.4496						

```
                             TIME =    28.0000
MAXIMUM  PORE PRESSURE RATIO =      .4073
AVERAGE  PORE PRESSURE RATIO =      .3290
GREATEST PORE PRESSURE RATIO =      .4073
```

EXCESS PORE WATER PRESSURE(I)

1	0.	2	16.7143	3	27.0680	4	33.7039	5	37.8346
6	40.0631	7	40.7346						

```
                             TIME =    31.5000
MAXIMUM  PORE PRESSURE RATIO =      .4275
AVERAGE  PORE PRESSURE RATIO =      .3448
GREATEST PORE PRESSURE RATIO =      .4275
```

EXCESS PORE WATER PRESSURE(I)

1	0.	2	17.4468	3	28.2680	4	35.2845	5	39.6660
6	42.0352	7	42.7504						

```
                             TIME =    35.0000
MAXIMUM  PORE PRESSURE RATIO =      .4455
AVERAGE  PORE PRESSURE RATIO =      .3588
GREATEST PORE PRESSURE RATIO =      .4455
```

EXCESS PORE WATER PRESSURE(I)

1	0.	2	18.0637	3	29.3601	4	36.6906	5	41.2954
6	43.7949	7	44.5507						

```
                             TIME =    38.5000
MAXIMUM  PORE PRESSURE RATIO =      .4617
AVERAGE  PORE PRESSURE RATIO =      .3715
GREATEST PORE PRESSURE RATIO =      .4617
```

EXCESS PORE WATER PRESSURE(I)

1	0.	2	18.6417	3	30.3244	4	37.9582	5	42.7642
6	45.3793	7	46.1714						

```
                         TIME =      42.0000
MAXIMUM  PORE PRESSURE RATIO =        .4764
AVERAGE  PORE PRESSURE RATIO =        .3829
GREATEST PORE PRESSURE RATIO =        .4764

EXCESS PORE WATER PRESSURE(I)

   1    0.          2   19.1493     3   31.2111     4   39.1053     5   44.0967
   6   46.8194      7   47.6449

                         TIME =      45.5000
MAXIMUM  PORE PRESSURE RATIO =        .4900
AVERAGE  PORE PRESSURE RATIO =        .3934
GREATEST PORE PRESSURE RATIO =        .4900

EXCESS PORE WATER PRESSURE(I)

   1    0.          2   19.6243     3   32.0125     4   40.1573     5   45.3173
   6   48.1384      7   48.9950

                         TIME =      49.0000
MAXIMUM  PORE PRESSURE RATIO =        .5024
AVERAGE  PORE PRESSURE RATIO =        .4031
GREATEST PORE PRESSURE RATIO =        .5024

EXCESS PORE WATER PRESSURE(I)

   1    0.          2   20.0539     3   32.7574     4   41.1250     5   46.4435
   6   49.3569      7   50.2423

                         TIME =      52.5000
MAXIMUM  PORE PRESSURE RATIO =        .5140
AVERAGE  PORE PRESSURE RATIO =        .4121
GREATEST PORE PRESSURE RATIO =        .5140

EXCESS PORE WATER PRESSURE(I)

   1    0.          2   20.4578     3   33.4441     4   42.0258     5   47.4909
   6   50.4908      7   51.4036

                         TIME =      56.0000
MAXIMUM  PORE PRESSURE RATIO =        .5249
AVERAGE  PORE PRESSURE RATIO =        .4206
GREATEST PORE PRESSURE RATIO =        .5249

EXCESS PORE WATER PRESSURE(I)
```

```
   1     0.          2   20.8316     3   34.0897     4   42.8676     5   48.4725
   6   51.5543       7   52.4929


                    TIME =     59.5000
MAXIMUM  PORE PRESSURE RATIO =    .5352
AVERAGE  PORE PRESSURE RATIO =    .4286
GREATEST PORE PRESSURE RATIO =    .5352

EXCESS PORE WATER PRESSURE(I)

   1     0.          2   21.1862     3   34.6954     4   43.6625     5   49.3989
   6   52.5590       7   53.5224


                    TIME =     63.0000
MAXIMUM  PORE PRESSURE RATIO =    .5450
AVERAGE  PORE PRESSURE RATIO =    .4361
GREATEST PORE PRESSURE RATIO =    .5450

EXCESS PORE WATER PRESSURE(I)

   1     0.          2   21.5206     3   35.2720     4   44.4167     5   50.2800
   6   53.5153       7   54.5026


                    TIME =     66.5000
MAXIMUM  PORE PRESSURE RATIO =    .5544
AVERAGE  PORE PRESSURE RATIO =    .4434
GREATEST PORE PRESSURE RATIO =    .5544

EXCESS PORE WATER PRESSURE(I)

   1     0.          2   21.8413     3   35.8218     4   45.1390     5   51.1240
   6   54.4324       7   55.4430


                    TIME =     70.0000
MAXIMUM  PORE PRESSURE RATIO =    .5635
AVERAGE  PORE PRESSURE RATIO =    .4504
GREATEST PORE PRESSURE RATIO =    .5635

EXCESS PORE WATER PRESSURE(I)

   1     0.          2   22.1490     3   36.3521     4   45.8348     5   51.9388
   6   55.3185       7   56.3519
```

```
                       TIME =        75.0000
MAXIMUM  PORE PRESSURE RATIO =         .4626
AVERAGE  PORE PRESSURE RATIO =         .3655
GREATEST PORE PRESSURE RATIO =         .5635

EXCESS PORE WATER PRESSURE(I)

   1    0.          2   16.8611     3   28.7870     4   37.0520     5   42.4118
   6   45.3650      7   46.2630


                       TIME =        80.0000
MAXIMUM  PORE PRESSURE RATIO =         .3765
AVERAGE  PORE PRESSURE RATIO =         .2979
GREATEST PORE PRESSURE RATIO =         .5635

EXCESS PORE WATER PRESSURE(I)

   1    0.          2   14.1969     3   23.5811     4   30.1186     5   34.4567
   6   36.8978      7   37.6489


                       TIME =        85.0000
MAXIMUM  PORE PRESSURE RATIO =         .3062
AVERAGE  PORE PRESSURE RATIO =         .2424
GREATEST PORE PRESSURE RATIO =         .5635

EXCESS PORE WATER PRESSURE(I)

   1    0.          2   11.3059     3   19.1891     4   24.5871     5   28.0889
   6   30.0310      7   30.6246


                       TIME =        90.0000
MAXIMUM  PORE PRESSURE RATIO =         .2495
AVERAGE  PORE PRESSURE RATIO =         .1974
GREATEST PORE PRESSURE RATIO =         .5635

EXCESS PORE WATER PRESSURE(I)

   1    0.          2    9.3619     3   15.6033     4   19.9708     5   22.8520
   6   24.4601      7   24.9523


                       TIME =        95.0000
MAXIMUM  PORE PRESSURE RATIO =         .2030
AVERAGE  PORE PRESSURE RATIO =         .1607
GREATEST PORE PRESSURE RATIO =         .5635

EXCESS PORE WATER PRESSURE(I)
```

1	0.	2	7.5174	3	12.7272	4	16.2874	5	18.6103
6	19.9066	7	20.3042						

TIME = 100.0000
MAXIMUM PORE PRESSURE RATIO = .1653
AVERAGE PORE PRESSURE RATIO = .1308
GREATEST PORE PRESSURE RATIO = .5635

EXCESS PORE WATER PRESSURE(I)

1	0.	2	6.1917	3	10.3389	4	13.2437	5	15.1508
6	16.2110	7	16.5350						

TIME = 105.0000
MAXIMUM PORE PRESSURE RATIO = .1346
AVERAGE PORE PRESSURE RATIO = .1065
GREATEST PORE PRESSURE RATIO = .5635

EXCESS PORE WATER PRESSURE(I)

1	0.	2	4.9909	3	8.4372	4	10.7913	5	12.3332
6	13.1956	7	13.4602						

TIME = 110.0000
MAXIMUM PORE PRESSURE RATIO = .1096
AVERAGE PORE PRESSURE RATIO = .0867
GREATEST PORE PRESSURE RATIO = .5635

EXCESS PORE WATER PRESSURE(I)

1	0.	2	4.0987	3	6.8523	4	8.7809	5	10.0432
6	10.7442	7	10.9585						

TIME = 115.0000
MAXIMUM PORE PRESSURE RATIO = .0892
AVERAGE PORE PRESSURE RATIO = .0706
GREATEST PORE PRESSURE RATIO = .5635

EXCESS PORE WATER PRESSURE(I)

1	0.	2	3.3114	3	5.5925	4	7.1509	5	8.1743
6	8.7467	7	8.9223						

```
                     TIME =   120.0000
MAXIMUM  PORE PRESSURE RATIO =      .0726
AVERAGE  PORE PRESSURE RATIO =      .0575
GREATEST PORE PRESSURE RATIO =      .5635

EXCESS PORE WATER PRESSURE(I)

   1    0.          2    2.7145     3    4.5419     4    5.8213     5    6.6569
   6    7.1212      7    7.2633
```

EARTHQUAKE ENGINEERING RESEARCH CENTER REPORTS

EERC 67-1 "Feasibility Study Large-Scale Earthquake Simulator Facility," by J. Penzien, J. G. Bouwkamp, R. W. Clough and D. Rea - 1967 (PB 187 905)

EERC 68-1 Unassigned

EERC 68-2 "Inelastic Behavior of Beam-to-Column Subassemblages Under Repeated Loading," by V. V. Bertero - 1968 (PB 184 888)

EERC 68-3 "A Graphical Method for Solving the Wave Reflection-Refraction Problem," by H. D. McNiven and Y. Mengi - 1968 (PB 187 943)

EERC 68-4 "Dynamic Properties of McKinley School Buildings," by D. Rea, J. G. Bouwkamp and R. W. Clough - 1968 (PB 187 902)

EERC 68-5 "Characteristics of Rock Motions During Earthquakes," by H. B. Seed, I. M. Idriss and F. W. Kiefer - 1968 (PB 188 338)

EERC 69-1 "Earthquake Engineering Research at Berkeley," - 1969 (PB 187 906)

EERC 69-2 "Nonlinear Seismic Response of Earth Structures," by M. Dibaj and J. Penzien - 1969 (PB 187 904)

EERC 69-3 "Probabilistic Study of the Behavior of Structures During Earthquakes," by P. Ruiz and J. Penzien - 1969 (PB 187 886)

EERC 69-4 "Numerical Solution of Boundary Value Problems in Structural Mechanics by Reduction to an Initial Value Formulation," by N. Distefano and J. Schujman - 1969 (PB 187 942)

EERC 69-5 "Dynamic Programming and the Solution of the Biharmonic Equation," by N. Distefano - 1969 (PB 187 941)

EERC 69-6 "Stochastic Analysis of Offshore Tower Structures," by A. K. Malhotra and J. Penzien - 1969 (PB 187 903)

EERC 69-7 "Rock Motion Accelerograms for High Magnitude Earthquakes," by H. B. Seed and I. M. Idriss - 1969 (PB 187 940)

EERC 69-8 "Sturctural Dynamics Testing Facilities at the University of California, Berkeley," by R. M. Stephen, J. G. Bouwkamp, R. W. Clough and J. Penzien - 1969 (PB 189 111)

Note: Numbers in parentheses are Accession Numbers assigned by the National Technical Information Service. Copies of these reports may be ordered from the National Technical Information Service, Springfield, Virginia 22151. Accession Numbers should be quoted on orders for reports.

EERC 69-9 "Seismic Response of Soil Deposits Underlain by Sloping Rock Boundaries," by H. Dezfulian and H. B. Seed - 1969 (PB 189 114)

EERC 69-10 "Dynamic Stress Analysis of Axisymmetric Structures Under Arbitrary Loading," by S. Ghosh and E. L. Wilson - 1969 (PB 189 026)

EERC 69-11 "Seismic Behavior of Multistory Frames Designed by Different Philosophies," by J. C. Anderson and V. V. Bertero - 1969 (PB 190 662)

EERC 69-12 "Stiffness Degradation of Reinforcing Concrete Structures Subjected to Reversed Actions," by V. V. Bertero, B. Bresler and H. Ming Liao - 1969 (PB 202 942)

EERC 69-13 "Response of Non-Uniform Soil Deposits to Travelling Seismic Waves," by H. Dezfulian and H. B. Seed - 1969 (PB 191 023)

EERC 69-14 "Damping Capacity of a Model Steel Structure," by D. Rea, R. W. Clough and J. G. Bouwkamp - 1969 (PB 190 663)

EERC 69-15 "Influence of Local Soil Conditions on Building Damage Potential During Earthquakes," by H. B. Seed and I. M. Idriss - 1969 (PB 191 036)

EERC 69-16 "The Behavior of Sands Under Seismic Loading Conditions," by M. L. Silver and H. B. Seed - 1969 (AD 714 982)

EERC 70-1 "Earthquake Response of Concrete Gravity Dams," by A. K. Chopra - 1970 (AD 709 640)

EERC 70-2 "Relationships Between Soil Conditions and Building Damage in the Caracas Earthquake of July 29, 1967," by H. B. Seed, I. M. Idriss, and H. Dezfulian - 1970 (PB 195 762)

EERC 70-3 "Cyclic Loading of Full Size Steel Connections," by E. P. Popov and R. M. Stephen - 1970 (Not available from NTIS)

EERC 70-4 "Seismic Analysis of the Charaima Building, Caraballeda, Venezuela," by Subcommittee of the SEAONC Research Committee, V. V. Bertero, P. F. Fratessa, S. A. Mahin, J. H. Sexton, A. C. Scordelis, E. L. Wilson, L. A. Wyllie, H. B. Seed, and J. Penzien, Chairman - 1970 (PB 201 455)

EERC 70-5 "A Computer Program for Earthquake Analysis of Dams," by A. K. Chopra - 1970 (AD 723 994)

EERC 70-6 "The Propagation of Love Waves Across Non-Horizontally Layered Structures," by J. Lysmer and L. A. Drake - 1970 (PB 197 896)

EERC 70-7 "Influence of Base Rock Characteristics on Ground Response," by J. Lysmer, H. B. Seed and P. B. Schnabel - 1970 (PB 197 897)

EERC 70-8 "Applicability of Laboratory Test Procedures for Measuring Soil Liquefaction Characteristics Under Cyclic Loading," by H. B. Seed and W. H. Peacock - 1970 (PB 198 016)

EERC 70-9 "A Simplified Procedure for Evaluating Soil Liquefaction Potential," by H. B. Seed and I. M. Idriss - 1970 (PB 198 009)

EERC 70-10 "Soil Moduli and Damping Factors for Dynamic Response Analysis," by H. B. Seed and I. M. Idriss - 1970 (PB 197 869)

EERC 71-1 "Koyna Earthquake and the Performance of Koyna Dam," by A. K. Chopra and P. Chakrabarti - 1971 (AD 731 496)

EERC 71-2 "Preliminary In-Situ Measurements of an Elastic Abosrption in Soils Using a Prototype Earthquake Simulator," by R. D. Borcherdt and P. W. Rodgers - 1971 (PB 201 454)

EERC 71-3 "Static and Dynamic Analysis of Inelastic Frame Structures," by F. L. Porter and G. H. Powell - 1971 (PB 210 135)

EERC 71-4 "Research Needs in Limit Design of Reinforced Concrete Structures," by V. V. Bertero - 1971 (PB 202 943)

EERC 71-5 "Dynamic Behavior of a High-Rise Diagonally Braced Steel Building," by D. Rea, A. A. Shah and J. G. Bouwkamp - 1971 (PB 203 584)

EERC 71-6 "Dynamic Stress Analysis of Porous Elastic Solids Saturated with Compressible Fluids," by J. Ghaboussi and E. L. Wilson - 1971 (PB 211 396)

EERC 71-7 "Inelastic Behavior of Steel Beam-to-Column Subassemblages," by H. Krawinkler, V. V. Bertero and E. P. Popov - 1971 (PB 211 335)

EERC 71-8 "Modification of Seismograph Records for Effects of Local Soil Conditions," by P. Schnabel, H. B. Seed and J. Lysmer - 1971 (PB 214 450)

EERC 72-1 "Static and Earthquake Analysis of Three Dimensional Frame and Shear Wall Buildings," by E. L. Wilson and H. H. Dovey - 1972 (PB 212 904)

EERC 72-2 "Accelerations in Rock for Earthquakes in the Western United States," by P. B. Schnabel and H. B. Seed - 1972 (PB 213 100)

EERC 72-3 "Elastic-Plastic Earthquake Response of Soil-Building Systems," by T. Minami and J. Penzien - 1972 (PB 214 868)

EERC 72-4 "Stochastic Inelastic Response of Offshore Towers to Strong Motion Earthquakes," by M. K. Kaul and J. Penzien - 1972 (PB 215 713)

EERC 72-5 "Cyclic Behavior of Three Reinforced Concrete Flexural Members with High Shear," by E. P. Popov, V. V. Bertero and H. Krawinkler - 1972 (PB 214 555)

EERC 72-6 "Earthquake Response of Gravity Dams Including Reservoir Interaction Effects," by P. Chakrabarti and A. K. Chopra - 1972 (AD 762 330)

EERC 72-7 "Dynamic Properties of Pine Flat Dam," by D. Rea, C.-Y. Liau and A. K. Chopra - 1972 (AD 763 928)

EERC 72-8 "Three Dimensional Analysis of Building Systems," by E. L. Wilson and H. H. Dovey - 1972 (PB 222 438)

EERC 72-9 "Rate of Loading Effects on Uncracked and Repaired Reinforced Concrete Members," by V. V. Bertero, D. Rea, S. Mahin and M. Atalay - 1972

EERC 72-10 "Computer Program for Static and Dynamic Analysis of Linear Structural Systems," by E. L. Wilson, K. J. Bathe, J. E. Peterson and H. H. Dovey - 1973 (PB 220 437)

EERC 72-11 "Literature Survey - Seismic Effects on Highway Bridges," by T. Iwasaki, J. Penzien and R. Clough - 1972 (PB 215 613)

EERC 72-12 "SHAKE--A Computer Program for Earthquake Response Analysis of Horizontally Layered Sites," by Per B. Schnabel, John Lysmer and H. Bolton Seed - 1972 (PB 220 207)

EERC 73-1 "Optimal Seismic Design of Multistory Frames," by V. V. Bertero and H. Kamil - 1973

EERC 73-2 "Analysis of Slides in the San Fernando Dams during the Earthquake of February 9, 1971," by H. B. Seed, K. L. Lee, I. M. Idriss and F. Makdisi - 1973

EERC 73-3 "Computer Aided Ultimate Load Design of Unbraced Multistory Steel Frames," by M. B. El-Hafez and G. J. Powell - 1973

EERC 73-4 "Experimental Investigation Into the Seismic Behavior of Critical Regions of Reinforced Concrete Components as Influenced by Moment and Shear," by M. Celebi and J. Penzien - 1973 (PB 215 884)

EERC 73-5 "Hysteretic Behavior of Epoxy-Repaired Reinforced Concrete Beams," by M. Celebi and J. Penzien - 1973

EERC 73-6 "General Purpose Computer Program for Inelastic Dynamic Response of Plane Structures," by A. Kanaan and G. H. Powell - 1973 (PB 221 260)

EERC 73-7 "A Computer Program for Earthquake Analysis of Gravity Dams Including Reservoir Interaction," by P. Chakrabarti and A. K. Chopra - 1973

EERC 73-8 "Seismic Behavior of Spandrel Frames - A Review and Outline for Future Research," by R. Razani and J. G. Bouwkamp - 1973

EERC 73-9 "Earthquake Analysis of Structure-Foundation Systems," by A. K. Vaish and A. K. Chopra - 1973

EERC 73-10 "Deconvolution of Seismic Respose for Linear Systems," by R. B. Reimer - 1973 (PB 227 197/AS)

EERC 73-11 "SAP IV Structure Analysis Program for Static and Dynamic Response of Linear Systems," by K.-J. Bathe, E. L. Wilson and F. E. Peterson - 1973 (PB 221 967)

EERC 73-12 "Analytical Investigations of the Seismic Response of Tall Flexible Highway Bridges," by W. S. Tseng and J. Penzien - 1973 (PB 227 816/AS)

EERC 73-13 "Earthquake Analysis of Multi-Story Buildings Including Foundation Interaction," by A. K. Chopra and J. A. Gutierrez - 1973 (PB 222 970)

EERC 73-14 "ADAP A Computer Program for Static and Dynamic Analysis of Arch Dams," by R. W. Clough, J. M. Raphael and S. Mojtahedi - 1973 (PB 223 763/AS)

EERC 73-15 "Cyclic Plastic Analysis of Structural Steel Joints," by R. B. Pinkney and R. W. Clough - 1973 (PB 226 843/AS)

EERC 73-16 "QUAD-4 A Computer Program for Evaluating the Seismic Response of Soil Structures by Variable Damping Finite Element Procedures," by I. M. Idriss, J. Lysmer, R. Hwang and H. B. Seed - 1973

EERC 73-17 "Dynamic Behavior of a Multi-Story Pyramid Shaped Building," by R. M. Stephen and J. G. Bouwkamp - 1973

EERC 73-18 "Effect of Different Types of Reinforcing on Seismic Behavior of Short Concrete Columns," by V. V. Bertero, J. Hollings, O. Kustu, R. M. Stephen and J. G. Bouwkamp - 1973

EERC 73-19 "Olive View Medical Center Material Studies, Phase I," by B. Bresler and V. Bertero - 1973

EERC 73-20 "Linear and Nonlinear Seismic Analysis Computer Programs for Long Multiple-Span Highway Bridges," by W. S. Tseng and J. Penzien - 1973

EERC 73-21 "Constitutive Models for Cyclic Plastic Deformation of Engineering Materials," by J. M. Kelly and P. P. Gillis - 1973 (PB 226 024/AS)

EERC 73-22 "DRAIN - 2D Users Guide," by G. H. Powell - 1973 (PB 227 016/AS)

EERC 73-23 "Earthquake Engineering at Berkeley - 1973" - 1973 (PB 226 033/AS)

EERC 73-24 "Seismic Input and Structural Response During the 1971 San Fernando Earthquake," by R. B. Reimer, R. W. Clough and J. M. Raphael - 1973

EERC 73-25 "Earthquake Response of Axisymmetric Tower Structures Surrounded by Water," by C. Y. Liaw and A. K. Chopra - 1973

EERC 73-26 "Investigation of the Failures of the Olive View Stair-towers During the San Fernando Earthquake and their Implications on Seismic Design," by V. V. Bertero and R. G. Collins - 1973

EERC 73-27 "Further Studies on Seismic Behavior of Steel Beam-Column Subassemblages," by V. V. Bertero, H. Krawinkler and E. P. Popov - 1973 (PB 234 172/AS)

EERC 74-1 "Seismic Risk Analysis," by C. S. Oliveira - 1974

EERC 74-2 "Settlement and Liquefaction of Sands Under Multi-Directional Shaking," by Robert Pyke, C. K. Chan and H. Bolton Seed - 1974

EERC 74-3 "Optimum Design of Earthquake Resistant Shear Buildings," by D. Rea, K. S. Pister, A. K. Chopra - 1974 (PB 231 172/AS)

EERC 74-4 "LUSH--A Computer Program for Complex Response Analysis of Soil-Structure Systems," by John Lysmer, Takekazu Udaka, H. Bolton Seed and Richard Hwang - 1974

EERC 74-5 "Sensitivity Analysis for Hysteretic Dynamic Systems: Applications to Earthquake Engineering," by D. Ray - 1974 (PB 233 213/AS)

EERC 74-6 "Soil-Structure Interaction Analyses for Evaluating Seismic Response," by H. B. Seed, J. Lysmer and R. Hwang - 1974

EERC 74-7 "Response of Radiation-Shielding Blocks to Earthquake Motions," by M. Aslam, W. G. Godden and D. T. Scalise - 1974

EERC 74-8 "Shaking Table Tests of a Steel Frame - A Progress Report," by R. W. Clough and David Tang - 1974

EERC 74-9 "Hysteretic Behavior of Reinforced Concrete Flexural Members with Special Web Reinforcement," by V. V. Bertero, E. P. Popov and T. Y. Wang - 1974

EERC 74-10 "Applications of Reliability-Based, Global Cost Optimization to Design of Earthquake Resistant Structures," by E. Vitiello and K. S. Pister - 1974

EERC 74-11 "Liquefaction of Gravelly Soils under Cyclic Loading Conditions," by R. T. Wong, H. B. Seed and C. K. Chan - 1974

EERC 74-12 "Site-Dependent Spectra for Earthquake-Resistant Design," by H. B. Seed, C. Ugas and J. Lysmer - 1974 (PB 240 953)

EERC 74-13 "Earthquake Simulator Study of a Reinforced Concrete Frame," by P. Hidalgo - 1974

EERC 74-14 "Nonlinear Earthquake Response of Concrete Gravity Dams," by N. Pal - 1974

EERC 74-15 "Modeling and Identification in Nonlinear Structural Dynamics, I - One Degree of Freedom Models," by N. Distefano and A. Rath - 1974 (PB 241 548)

EERC 75-1 "Determination of Seismic Design Criteria for the Dumbarton Bridge Replacement Structure, Vol. I: Description, Theory and Analytical Modeling of Bridge and Parameters," by F. Baron and S.-H. Tang - 1975

EERC 75-2 "Determination of Seismic Design Criteria for the Dumbarton Bridge Replacement Structure, Vol. 2: Numerical Studies and Establishment of Seismic Design Criteria," by F. Baron and S.-H. Tang - 1975

EERC 75-3 "Seismic Risk Analysis for a Site and a Metropolitan Area," by C. S. Oliveira - 1975

EERC 75-4 "Analytical Investigations of Seismic Response of Short, Single or Multiple-Span Highway Bridges," by Ma-chi Chen and J. Penzien - 1975 (PB 241 454)

EERC 75-5 "An Evaluation of Some Methods for Predicting Seismic Behavior of Reinforced Concrete Buildings," by Stephen A. Mahin and V. V. Bertero - 1975

EERC 75-6 "Earthquake Simulator Study of a Steel Frame Structure, Vol. I: Experimental Results," by R. W. Clough and David T. Tang - 1975

EERC 75-7 "Dynamic Properties of San Bernardino Intake Tower," by Dixon Rea, C-Y. Liaw and Anil K. Chopra - 1975

EERC 75-8 "Seismic Studies of the Atriculation for the Dumbarton Bridge Replacement Structure, Vol. I: Description, Theory and Analytical Modeling of Bridge and Components," by F. Baron and R. E. Hamati - 1975

EERC 75-9 "Seismic Studies of the Articulation for the Dumbarton Bridge Replacement Structure, Vol. 2: Numerical Studies of Steel and Concrete Girder Alternates," by F. Baron and R. E. Hamati - 1975

EERC 75-10 "Static and Dynamic Analysis of Nonlinear Structures," by Digambar P. Mondkar and Graham H. Powell - 1975

EERC 75-11 "Behavior of Reinforced Concrete Deep Beam-Column Subassemblages Under Cyclic Loads," by O. Kustu and J. G. Bouwkamp - 1975

EERC 75-12 "Earthquake Engineering Research Center Library Printed Catalog," - 1975

EERC 75-13 "Three Dimensional Analysis of Building Systems," Extended Version, by E. L. Wilson, J. P. Hollings, and H. H. Dovey - 1975

EERC 75-14 "Determination of Soil Liquefaction Characteristics by Large-Scale Laboratory Tests," by Pedro De Alba, Clarence K. Chan and H. Bolton Seed - 1975

EERC 75-15 "A Literature Survey - Comprehensive, Tensile, Bond and Shear Strength of Masonry," by Ronald L. Mays and Ray Clough - 1975

EERC 75-16 "Hysteretic Behavior of Ductile Moment Resisting Reinforced Concrete Frame Components," by V. V. Bertero and E. P. Popov - 1975

EERC 75-17 "Relationships Between Maximum Acceleration, Maximum Velocity, Distance from Source and Local Site Conditions for Moderately Strong Earthquakes," by H. Bolton Seed, Ramesh Murarka, John Lysmer and I. M. Idriss - 1975

EERC 75-18 "The Effects of Method of Sample Preparation on the Cyclic Stress-Strain Behavior of Sands," by J. Paul Mulilis, Clarence K. Chan and H. Bolton Seed - 1975

EERC 75-19 "The Seismic Behavior of Critical Regions of Reinforced Concrete Components as Influenced by Moment, Shear and Axial Force," by B. Atalay and J. Penzien - 1975

EERC 75-20 "Dynamic Properties of an Eleven Story Masonry Building," by R. M. Stephen, J. P. Hollings, J. G. Bouwkamp and D. Jurukovski - 1975

EERC 75-21 "State-of-the-Art in Seismic Shear Strength of Masonry - An Evaluation and Review," by Ronald L. Mayes and Ray W. Clough - 1975

EERC 75-22 "Frequency Dependencies Stiffness Matrices for Viscoelastic Half-Plane Foundations," by Anil K. Chopra, P. Chakrabarti and Gautam Dasgupta - 1975

EERC 75-23 "Hysteretic Behavior of Reinforced Concrete Framed Walls," by T. Y. Wong, V. V. Bertero and E. P. Popov - 1975

EERC 75-24 "Testing Facility for Subassemblages of Frame-Wall Structural Systems," by V. V. Bertero, E. P. Popov and T. Endo - 1975

EERC 75-25 "Influence of Seismic History on the Liquefaction Characteristics of Sands," by H. Bolton Seed, Kenji Mori and Clarence K. Chan - 1975

EERC 75-26 "The Generation and Dissipation of Pore Water Pressures During Soil Liquefaction," by H. Bolton Seed, Phillippe P. Martin and John Lysmer - 1975

EERC 75-27 "Identification of Research Needs for Improving a Seismic Design of Building Structures," by V. V. Bertero - 1975

EERC 75-28 "Evaluation of Soil Liquefaction Potential during Earthquakes," by H. Bolten Seed, I. Arango and Clarence K. Chan 1975

EERC 75-29 "Representation of Irregular Stress Time Histories by Equivalent Uniform Stress Series in Liquefaction Analyses," by H. Bolton Seed, I. M. Idriss, F. Makdisi and N. Banerjee 1975

EERC 75-30 "FLUSH - A Computer Program for Approximate 3-D Analysis of Soil-Structure Interaction Problems," by J. Lysmer, T. Udaka, C.-F. Tsai and H. B. Seed - 1975

EERC 75-31 "ALUSH - A Computer Program for Seismic Response Analysis of Axisymmetric Soil-Structure Systems," by E. Berger, J. Lysmer and H. B. Seed - 1975

EERC 75-32 "TRIP and TRAVEL - Computer Programs for Soil-Structure Interaction Analysis with Horizontally Travelling Waves," by T. Udaka, J. Lysmer and H. B. Seed - 1975

EERC 75-33 "Predicting the Performance of Structures in Regions of High Seismicity," by J. Penzien - 1975

EERC 75-34 "Efficient Finite Element Analysis of Seismic Structure - Soil - Direction," by J. Lysmer, H. Bolton Seed, T. Udaka, R. N. Hwang and C.-F. Tsai - 1975

EERC 75-35 "The Dynamic Behavior of a First Story Girder of a Three-Story Steel Frame Subjected to Earthquake Loading," by Ray W. Clough and Lap-Yan Li - 1975

EERC 75-36 "Earthquake Simulator Study of a Steel Frame Structure, Volume II - Analytical Results," by David T. Tang - 1975

EERC 75-37 "ANSR-I General Purpose Computer Program for Analysis of Non-Linear Structural Response," by Digambar P. Mondkar and Graham H. Powell - 1975

EERC 75-38 "Nonlinear Response Spectra for Probabilistic Seismic Design and Damage Assessment of Reinforced Concrete Structures," by Masaya Murakami and Joseph Penzien - 1975

EERC 75-39 "Study of a Method of Feasible Directions for Optimal Elastic Design of Framed Structures Subjected to Earthquake Loading," by N. D. Walker and K. S. Pister - 1975

EERC 75-40 "An Alternative Representation of the Elastic-Viscoelastic Analogy," by Gautam Dasgupta and Jerome L. Sackman - 1975

EERC 75-41 "Effect of Multi-Directional Shaking on Liquefaction of Sands," by H. Bolton Seed, Robert Pyke and Geoffrey R. Martin - 1975

EERC 76-1 "Strength and Ductility Evaluation of Existing Low-Rise Reinforced Concrete Buildings - Screening Method," by Tsuneo Okada and Boris Bresler - 1976

EERC 76-2 "Experimental and Analytical Studies on the Hysteretic Behavior of Reinforced Concrete Rectangular and T-Beams," by Shao-Yeh Marshall Ma, Egor P. Popov and Vitelmo V. Bertero - 1976

EERC 76-3 "Dynamic Behavior of a Multistory Triangular-Shaped Building," by J. Petrovski, R. M. Stephen, E. Gartenbaum and J. G. Bouwkamp - 1976

EERC 76-4 "Earthquake Induced Deformations of Earth Dams," by Norman Serff and H. Bolton Seed - 1976

EERC 76-5 "Analysis and Design of Tube-Type Tall Building Structures," by H. de Clercq and G. H. Powell - 1976

EERC 76-6 "Time and Frequency Domain Analysis of Three-Dimensional Ground Motions, San Fernando Earthquake," by Tetsuo Kubo and Joseph Penzien - 1976

EERC 76-7 "Expected Performance of Uniform Building Code Design Masonry Structures," by R. L. Mayes, Y. Omote, S. W. Chen and R. W. Clough - 1976

EERC 76-8 "Cyclic Shear Tests on Concrete Masonry Piers," R. L. Mayes, Y. Omote and R. W. Clough - 1976

EERC 76-9 "A Substructure Method for Earthquake Analysis of Structure-Soil Interaction," by Jorge Alberto Gutierrez and Anil K. Chopra - 1976

EERC 76-10 "Stabilization of Potentially Liquefiable Sand Deposits Using Gravel Drain Systems," by H. Bolton Seed, and John R. Booker - 1976

BIBLIOGRAPHIC DATA SHEET	1. Report No. EERC 76-10	2.	3. Recipient's Accession No.

4. Title and Subtitle

"Stabilization of Potentially Liquefiable Sand Deposits using Gravel Drain Systems"

5. Report Date: April 1976

6.

7. Author(s)

H. Bolton Seed and John R. Booker

8. Performing Organization Rept. No. 76-10

9. Performing Organization Name and Address

Earthquake Engineering Research Center
University of California, Berkeley
1301 S. 46th Street
Richmond, California 94804

10. Project/Task/Work Unit No.

11. Contract/Grant No. ENV75-21875

12. Sponsoring Organization Name and Address

National Science Foundation
1800 G Street
Washington, D. C. 20550

13. Type of Report & Period Covered

14.

15. Supplementary Notes

16. Abstracts

In many cases, the installation of a system of vertical columnar drains offers an attractive and economical procedure for stabilizing an otherwise potentially liquefiable sand deposit. In fact, the method has already been used in one case involving the construction of stone columns in a relatively loose sand deposit and it is currently being proposed for stabilization of a medium dense sand layer which is known to have developed some degree of liquefaction in a recent earthquake but which appears to be too dense for stabilization by further densification using currently available procedures.

The report presents a simplified theory which provides a convenient basis for evaluating the possible effectiveness of a gravel drain system in such cases. Where appropriate, additional analyses may readily be made using the computer program LARF described in the report but for most practical cases, it is believed that the results presented in chart form will provide an adequate basis for design and selection of a suitable drain system for effective stabilization of potentially liquefiable sand deposits.

17b. Identifiers/Open-Ended Terms

17c. COSATI Field/Group

18. Availability Statement	19. Security Class (This Report)	21. No. of Pages
Release Unlimited	UNCLASSIFIED	
	20. Security Class (This Page) UNCLASSIFIED	